Prepared for publication in *RSC Advances*

October 10, 2014

Exploring Photophysical Properties of Metal-free Coumarin Sensitizers: An Efficient Strategy to Improve Performance of Dye-sensitized Solar

Jinghui Wang,[a] Ming Li,[a, b] Dan Qi,[a] Wei Shen,[a] Rongxing He[*a, b] and Sheng Hsien Lin[c]

[a] *School of Chemistry and Chemical Engineering, Southwest University, Chongqing 400715, China; E-mail: herx@swu.edu.cn*

[b] *Education Ministry Key Laboratory on Luminescence and Real-Time Analysis, Southwest University, Chongqing 400715, China*

[c] *Department of Applied Chemistry, Institute of Molecular Science and Center for Interdisciplinary Molecular Science, National Chiao-Tung University, Hsinchu 300, Taiwan*

Detailed discussion to confirm the significant role of π-spacer of model dyes in promoting the performance of DSSCs

Free dye

In this work, we firstly considered four parent coumarin-based sensitizers (NKX-2311, NKX-2677, NKX-2700 and NKX-2883) and combined the calculated results with experimental findings to confirm the significant role of π-spacer of sensitizers in promoting the J_{sc} of DSSCs. The only difference of structures for these four dyes is the π-spacers, as shown in Fig 1. As shown in Equation 1, the J_{sc} is determined by four factors: light harvest efficiency (φ_{LHE}), electron injection efficiency (φ_{inject}), charge collection efficiency (φ_{cc}) and the regeneration efficiency (φ_{reg}).We firstly discuss the function of different π-spacers in improving light harvesting efficiency (φ_{LHE}). Usually, the φ_{LHE} is closely related with oscillator strength (f) of coumarin dye associated to the λ, and it can be written as:

$$\varphi_{LHE} = 1 - 10^{-f} \quad (1)$$

The maximum absorption wavelength (λ_{max}) and corresponding oscillation strength (f) and light harvesting efficiency (φ_{LHE}) for NKX-2311, NKX-2677, NKX-2700, and NKX-2883 are listed in Table 6S. As the π-spacer of NKX-2311 changes from vinylene unit to couple of thiophene moieties of NKX-2677, the red-shifted and strengthened Q band can be obtained, eventually resulting in higher light harvesting efficiency. Compared with NKX-2677, however, NKX-2700 and NKX-2883 display wider visible absorption bands, which are ascribed to the facts that the additional vinylene unit in NKX-2700 structure expands the π-system, and the auxiliary electron withdrawing -CN unit in NKX-2883 facilitates electron migration to the acceptor unit. Obviously, when the π-spacer of dye is expanded with introduction of different groups, the location of λ_{max} will red shift to a certain extent and follows the order of NKX-2311(459 nm) < NKX-2677 (508 nm) < NKX-2700 (527 nm) < NKX-2883(536 nm). Meanwhile, the values of φ_{LHE} (λ_{max}) comply with the sequence of NKX-2311(0.983) < NKX-2677 (0.986) < NKX-2700 (0.996) ≈ NKX-2883 (0.994). Consequently, it is undoubtedly that the absorption of coumarin-based dyes can be extended to long-wavelength region leading to an improved spectral overlap with the solar spectrum, and the light-capturing ability can be enhanced through proper modification of the π-spacer, which would further improve the φ_{LHE} for high short-circuit current density (J_{sc}).

Generally, if the charge recombination process is effectively suppressed, the electron collection efficiency (φ_{cc}) will be improved. Clifford *et al* reported that the increase of link length of π-spacer could slow down the electron recombination rate. In our research, the length of π-spacers of these four model dyes follows the order of NKX-2311(3.796 Å) < NKX-2677 (9.215 Å) < NKX-2700 (11.674 Å) ≈ NKX-2883 (11.225 Å). That is, the expansion of π-spacer will effectively inhibit the charge recombination efficiency, thereby improving electron collection efficiency (φ_{cc}). In addition, a favorable charge separation will facilitate electronic injection from excited dye to semiconductor surface, and then promote the photogenerated charge to be transported to the electrodes. Consequently, effective electron collection efficiency requires a good intramolecular charge separation with photoexcitation occurring. As shown in Table 1, the extension of the π-spacers prompts the electron densities of HOMOs of NKX-2677, NKX-2700 and NKX-2883 to distribute mainly on their donors (HOMO of NKX-2311 is delocalized over the whole dye molecule). Because of the almost same distribution of LUMOs' electron densities for these four dyes, the difference in HOMOs indicates more effective charge separation for NKX-2677, NKX-2700 and NKX-2883 comparing with NKX-2311, which leads to higher φ_{cc} of NKX-2677, NKX-2700 and NKX-2883. Thus, extending the π-spacer of dye with diverse groups not only retards the charge recombination efficiency, but also improves charge separation for high electron collection efficiency (φ_{cc}).

Besides, the regeneration efficiency (φ_{reg}) can be evaluated by the driver force of dye regeneration. The driver force for dye regeneration is represented by HOMO level of sensitizers. From Table 4, the HOMO levels of the model dyes are decreased slightly with the expansion of π-spacers, which implies the modification of π-spacers has slight effect on the performance of regeneration. As we known, the electron injection efficiency, φ_{inject}, depends on the competition between electron injection and charge recombination. Calculations shown that the driver force (see Table 4) for electron injection of these four dyes is sufficiently high, this induces the effective electron transfer from dye to semiconductor surface. Meanwhile, the charge recombination process is effectively suppressed by extending the linker of dyes. As a consequence, more effective electron injection can be obtained by modifying π-spacer of dyes.

Owing to broader absorption band in the NIR region and higher φ_{LHE}, more effective charge separation and slower charge recombination, the values of J_{sc} for NKX-2677, NKX-2700 and NKX-2883 are increased greatly relative to that of NKX-2311, indicating higher η for the DSSCs based on NKX-2677, NKX-2700 and NKX-2883. The present results are in good agreement with

the experiment findings. Undoubtedly, the performance of DSSCs can be improved through appropriate modification of dye structure with suitable π-spacer.

dye/ TiO_2 complexes

The simulated absorption spectra of NKX-2311/TiO_2, NKX-2677/TiO_2, NKX-2700/TiO_2 and NKX-2883/TiO_2 complexes are shown in Figures 1S-3S. Compared with the four isolated dyes (NKX-2311, NKX-2677, NKX-2700 and NKX-2883), the four dye-titania complexes achieve slight red-shift and broadening of the absorption peaks (the maximum absorption peaks are red-shifted by ~55, ~31, ~32 and ~20 nm, respectively, see Figure 1S and Table 4S), which are ascribed to the increased delocalization of the LUMO orbitals of the conjugated frameworks. Compared with NKX-2311/TiO_2, one of the most remarkable absorption features of the other complexes is the red-shifted bands, and they complied with the sequence of NKX-2311(514 nm) < NKX-2677 (539 nm) < NKX-2700 (559 nm) ≈ NKX-2883 (556 nm). This means that the extension of the length of π-space of dye could directly influence the absorption spectra of dye-titania complexes. Furthermore, the modification of the coumarin dye with various π-spacers significantly affects the oscillator strength of dye-titania complex. As listed in Table 4S, the oscillator strengths (*f*) of these four dye-titania complexes are enhanced (*f*=2.025, 2.210, 2.710 and 2.627 for NKX-2311/TiO_2, NKX-2677/TiO_2, NKX-2700/TiO_2 and NKX-2883/TiO_2), which subsequently improves the light harvesting efficiency of these complexes. Therefore, proper modification of the bridge of free dyes would directly improve the optical performance of dye-titania complexes. It is notable that no new bands are observed in the absorption spectra of the four dye-titania complexes relative to the four isolated dyes, indicating in present case the electron injection should adopt the indirect mechanism from donor of dye to semiconductor surface via acceptor (π-spacer and anchor groups).

The absorption spectra for these four complexes consist of many photo-excitations. Some of these excitations having relatively high oscillator strength are presented in Table 4S. For these four complexes, most of these photo-excitations originate from HOMO and HOMO-1 except NKX-2311(only from HOMO). The electron densities of HOMO and HOMO-1 are mainly localized on dye part of the complexes and are similar to the HOMO and HOMO-1 of isolated dyes, as shown in Figures 5S-7S. From Table 4S, the unoccupied orbitals that participate in the major excitations come from LUMO. Besides, there are some other molecular orbitals involved in the major excitations, such as LUMO+1 and LUIMO+16 of NKX-2677/TiO_2 complex. Among these unoccupied orbitals, LUMO shows highest contribution and is shown in Figure 5S. Remarkably, for LUMO orbital of these four complexes, only a few electron densities are delocalized on the cluster, indicating a weak interaction between excited dye and the surface of TiO_2, which favors the indirect mechanism for electron injection again.

After binding to titanium there is a redistribution of energy levels. The computed Kohn-Sham orbital energy levels for isolated dyes, $(TiO_2)_{16}$ cluster and dye/TiO_2 complexes are presented in Figure 4. The green line represents localization of molecular orbital both on the dye and the surface, blue denotes localization of molecular orbital on TiO_2 and red represents localization of molecular orbital on dyes. As reported in previous studies, the higher the LUMO is located in the semiconductor conduction band, the more efficient the electron injection is. From Figure 4, for all complexes, the LUMO is higher relative to the lower edge of the TiO_2 conduction band, which makes the electron injection be easy. As we have testified before, the absorption properties of NKX-2883 are comparable to those of NKX-2700, the former is even more outstanding. However, the η of NKX-2883-based DSSCs is slightly lower than that of NKX-2700-based DSSCs because the LUMO of NKX-2883/TiO_2 complex is relatively lower that of NKX-2700/TiO_2 complex, eventually reducing the efficiency of electron injection of NKX-2883. In addition, the partial and total densities of states for absorbed dyes have been calculated (Figure 4S). We notice that for all complexes, their unoccupied molecular orbitals have small overlap with the conduction band of TiO_2, and the overlap is slightly improved with the alteration of the π-spacer of dyes, indicating weak electronic coupling between dyes and TiO_2. It confirms again that the extension of the length of π-bridge with thienyl, vinylene or -CN groups has important influence on electronic coupling between dyes and TiO_2.

Overall, for these four systems, the absorption properties of dye/TiO_2 complexes are closely related to those of their free dyes. The extension of π-space of dyes with different groups effectively improves the optical performance of dye/TiO_2 complexes. Thus, rationally modification of the π-spacer can improve absorption spectra, re-shift orbital energy levels, and further boosts the performance of DSSCs.

Figure Captions

Fig. 1S (a) Simulated optical absorption for free sensitizers (b) Simulated absorption spectra for dyes absorbed on $Ti_{16}O_{32}$ cluster. The absorption spectra are simulated using M062X functional with 6-31g(d,p) basis set

Fig. 2S (a) Simulated optical absorption for free sensitizers (b) Simulated absorption spectra for dyes absorbed on $Ti_{16}O_{32}$ cluster. The absorption spectra are simulated using B3LYP functional with 6-31g(d,p) basis set

Fig. 3S (a) Simulated optical absorption for free sensitizers (b) Simulated absorption spectra for dyes absorbed on $Ti_{16}O_{32}$ cluster. The absorption spectra are simulated using PBE0 functional with 6-31g(d,p) basis set

Fig. 4S Total densities of states (TDOS) and partial densities of states (PDOS) for the eight coumarin-based dyes (the blue dashed line corresponds to TDOS, the red full line corresponds to TiO_2 (PDOS), and the black line corresponds to dye (PDOS)).

Fig. 5S Molecular orbitals relevant during photoexcitation for: 2311/TiO_2, 2677/TiO_2, 2700/TiO_2, 2883/TiO_2, 2883-P1/TiO_2, 2883-P2/TiO_2, 2883-Q1/TiO_2 and 2883-Q2/TiO_2 complexes. (M062X)

Fig. 6S Molecular orbitals relevant during photoexcitation for: 2311/TiO_2, 2677/TiO_2, 2700/TiO_2, 2883/TiO_2, 2883-P1/TiO_2, 2883-P2/TiO_2, 2883-Q1/TiO_2 and 2883-Q2/TiO_2 complexes. (B3LYP）

Fig. 7S Molecular orbitals relevant during photoexcitation for: 2311/TiO_2, 2677/TiO_2, 2700/TiO_2, 2883/TiO_2, 2883-P1/TiO_2, 2883-P2/TiO_2, 2883-Q1/TiO_2 and 2883-Q2/TiO_2 complexes. (PBE0)

Fig. 8S Frontier molecular orbital spatial distribution for free dyes (B3LYP)

Fig. 9S Frontier molecular orbital spatial distribution for free dyes (PBE0)

Fig. 10S Calculated UV/Vis absorption spectra four series sensitizers in ethanol solution obtained by using B3LYP functional with 6-31G(d,p) basis set, (a) NKX-2677, NKX-2677-P1 and NKX-2677-P2; (b) NKX-2700, NKX-2700-P1 and NKX-2700-P2; (c) NKX-2883, NKX-2883-P1 and NKX-2883-P2; (d) NKX-2883, NKX-2883-Q1 and NKX-2883-Q2

Fig. 11S Calculated UV/Vis absorption spectra four series sensitizers in ethanol solution obtained by using PBE0 functional with 6-31G(d,p) basis set, (a) NKX-2677, NKX-2677-P1 and NKX-2677-P2; (b) NKX-2700, NKX-2700-P1 and NKX-2700-P2; (c) NKX-2883, NKX-2883-P1 and NKX-2883-P2; (d) NKX-2883, NKX-2883-Q1 and NKX-2883-Q2

Fig. 12S Molecular orbital energy level (eV) diagram of (column 1) 2311/TiO_2 complex, (column 2) NKX-2311 dye, (column 3) 2677/TiO_2 complex, (column 4) NKX-2677 dye, (column 5) 2700/TiO_2 complex, (column 6) NKX-2700, (column 7) 2883/TiO_2 complex, (column 8) NKX-2883 dye, (column 9) isolated TiO_2, (column 10) NKX-2883-P1 dye, (column 11) 2883-P1/TiO_2 complex, (column 12) NKX-2883-P2 dye, (column 13) 2883-P2/TiO_2 complex, (column 14) NKX-2883-Q1 dye, (column 15) NKX-2883-Q1/TiO_2 complex, (column 16) NKX-2883-Q2 dye, (column 17) 2883-Q2/TiO_2 complex in ethanol solution. Green represents localization of molecular orbital both on the dye and the surface. Blue represents localization of molecular orbital on TiO_2. Red represents localization of molecular orbital on dyes (B3LYP)

Table Captions

Table 1S Transition energies (in eV) of S_0-S_1 transition for NKX-23111, NKX-2677, KNX-2700 and NKX-2883 coumarin dyes in ethanol solution with B3LYP/6-31g(d,p) geometries

Table 2S The HOMO energy levels (in eV) and corresponding oxidized potential (vs NHE, in eV) of ground state ($E_{ox(dye)}$) for NKX-2311, NKX-2677, NKX-2700, and NKX-2883. All values are calculated with B3LYP/6-31g(d,p) geometries

Table 3S Transition energies (in eV) of S_0-S_1 transition for dyes (NKX-23111, NKX-2677, KNX-2700 and NKX-2883) in ethanol solution. Geometries structures are optimized with different functionals.

Table 4S Electronic transition data obtained by TD-M062X/6-31g(d,p) level for all free dyes and dye-titania complexes in ethanol solution with B3LYP/6-31g(d,p) geometries

Table 5S Estimated $\Delta G_{(aq)}$, ΔG^0 , ΔE_{ver}, $E_{ox(dye)}$, ΔG_{reg}, f and LHE for all coumarin sensitizers. All calculation is obtained by M062X functional with b-31g(d,p) basis set

Table 6S Maximum absorption wavelength (λ_{max}) and the corresponding oscillation strength (f) and light harvest efficiency (φ_{LHE}) for NKX-2311, NKX-2677, NKX-2700, and NKX-2883

Table 7S Estimated $\Delta G_{(aq)}$, ΔG^0 , ΔE_{ver}, $E_{ox(dye)}$, ΔG_{reg}, f and LHE for all coumarin sensitizers. All calculation is obtained by B3LYP functional with b-31g(d,p) basis set

Table 8S Electronic transition data obtained by TD-B3LYP/6-31g(d,p) level for all free dyes and dye-titania complexes in ethanol solution with B3LYP/6-31g(d,p) geometries

Table 9S Electronic transition data obtained by TD-PBE0/6-31g(d,p) level for all free dyes and dye-titania complexes in ethanol solution with B3LYP/6-31g(d,p) geometries

Table 10S Electron density difference plots of electronic transition $S_0 \rightarrow S_1$ for each coumarin dyes performed in ethanol solution using the B3LYP functional with 6-31G(d,p) basis set. L is the electron transfer distance (Å); Δe is the fraction of electron exchange ($|e^-|$), Ω is overlaps between the regions of density depletion and increment. (Isovalue: 4×10^{-4} e au^{-3})

Table 11S Electron density difference plots of electronic transition $S_0 \rightarrow S_1$ for each coumarin dyes performed in ethanol solution using the PBE0 functional with 6-31G(d,p) basis set. L is the electron transfer distance (Å); Δe is the fraction of electron exchange ($|e^-|$), Ω is overlaps between the regions of density depletion and increment. (Isovalue: 4×10^{-4} e au^{-3})

Table 12S Electron density difference plots of electron transitions with oscillation strength larger than 0.1 for all dyes using M062X functional

Table 13S Electron density difference plots of electron transitions with oscillation strength larger than 0.1 for all dyes using B3LYP functional

Table 14S Electron density difference plots of electron transitions with oscillation strength larger than 0.1 for all dyes using PBE0 functional

Table 15S Calculated HOMO, LUMO energy levels (eV) of all sensitizers and the HOMO, LUMO energy levels (eV) of the donor (coumarin343) and the acceptor (conjugated π-spacer and anchoring group) fragments of all sensitizer obtained by B3LYP functional

Table 16S Calculated HOMO, LUMO energy levels (eV) of all sensitizers and the HOMO, LUMO energy levels (eV) of the donor (coumarin343) and the acceptor (conjugated π-spacer and anchoring group) fragments of all sensitizer obtained by M062X functional

Table 17S Molecular orbital composition (in %) of the highest occupied and two lowest unoccupied molecular orbital of the twelve coumarin sensitizers performed in ethanol solvent using B3LYP functional and the 6-31G(d,p) basis set.

Table 18S Molecular orbital composition (in %) of the highest occupied and two lowest unoccupied molecular orbital of the twelve coumarin sensitizers performed in ethanol solvent using PBE0 functional and the 6-31G(d,p) basis set.

Table 19S Estimated energy (a.u) of the oxidized coumarin dyes in ethanol solvent using PBE0 functional and the 6-31G(d,p) basis set

Table 20S Estimated energy(a.u) of the oxidized coumarin dyes in ethanol solvent using B3LYP functional and the 6-31G(d,p) basis set

Table 21S Estimated energy (a.u) of the oxidized coumarin dyes in ethanol solvent using M062X functional and the 6-31G(d,p) basis set

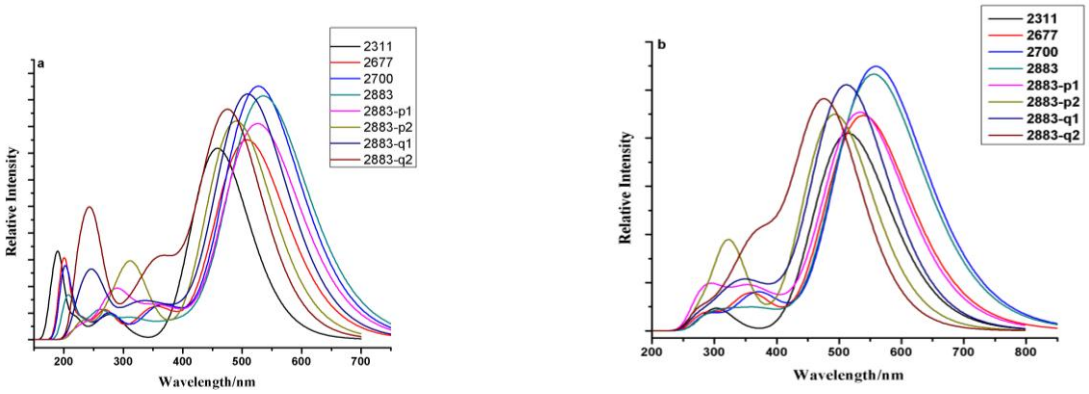

Fig. 1S (a) Simulated optical absorption for free sensitizers (b) Simulated absorption spectra for dyes absorbed on $Ti_{16}O_{32}$ cluster. The absorption spectra are simulated using M062X functional with 6-31G(d,p) basis set

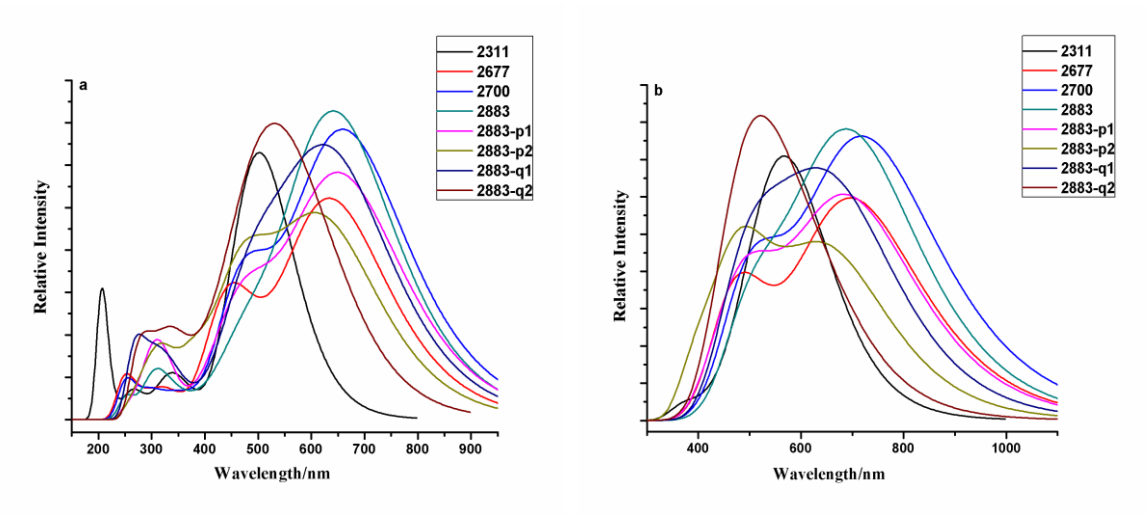

Fig. 2S (a) Simulated optical absorption for free sensitizers (b) Simulated absorption spectra for dyes absorbed on $Ti_{16}O_{32}$ cluster. The absorption spectra are simulated using B3LYP functional with 6-31G(d,p) basis set.

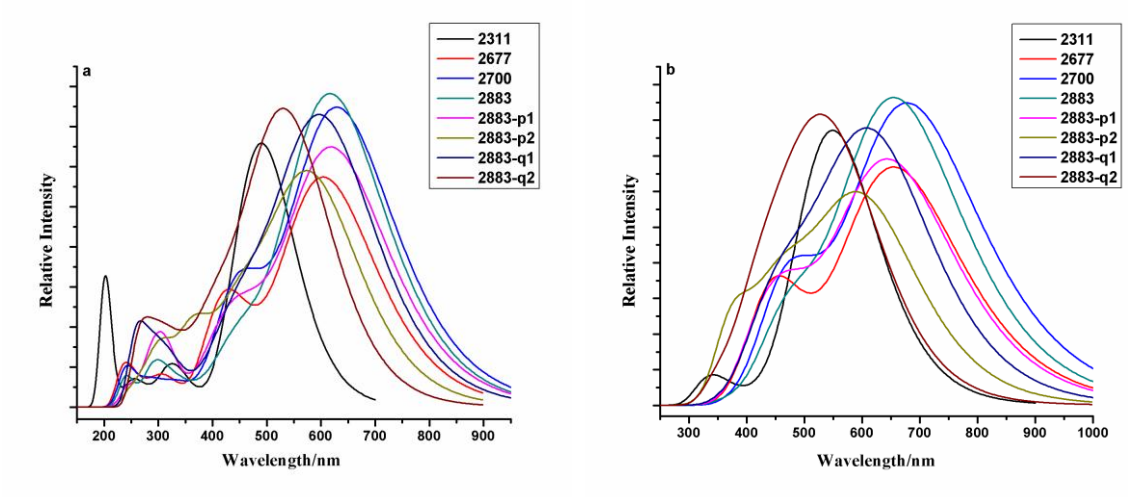

Fig. 3S (a) Simulated optical absorption for free sensitizers (b) Simulated absorption spectra for dyes absorbed on $Ti_{16}O_{32}$ cluster. The absorption spectra are simulated using PBE0 functional with 6-31G(d,p) basis set.

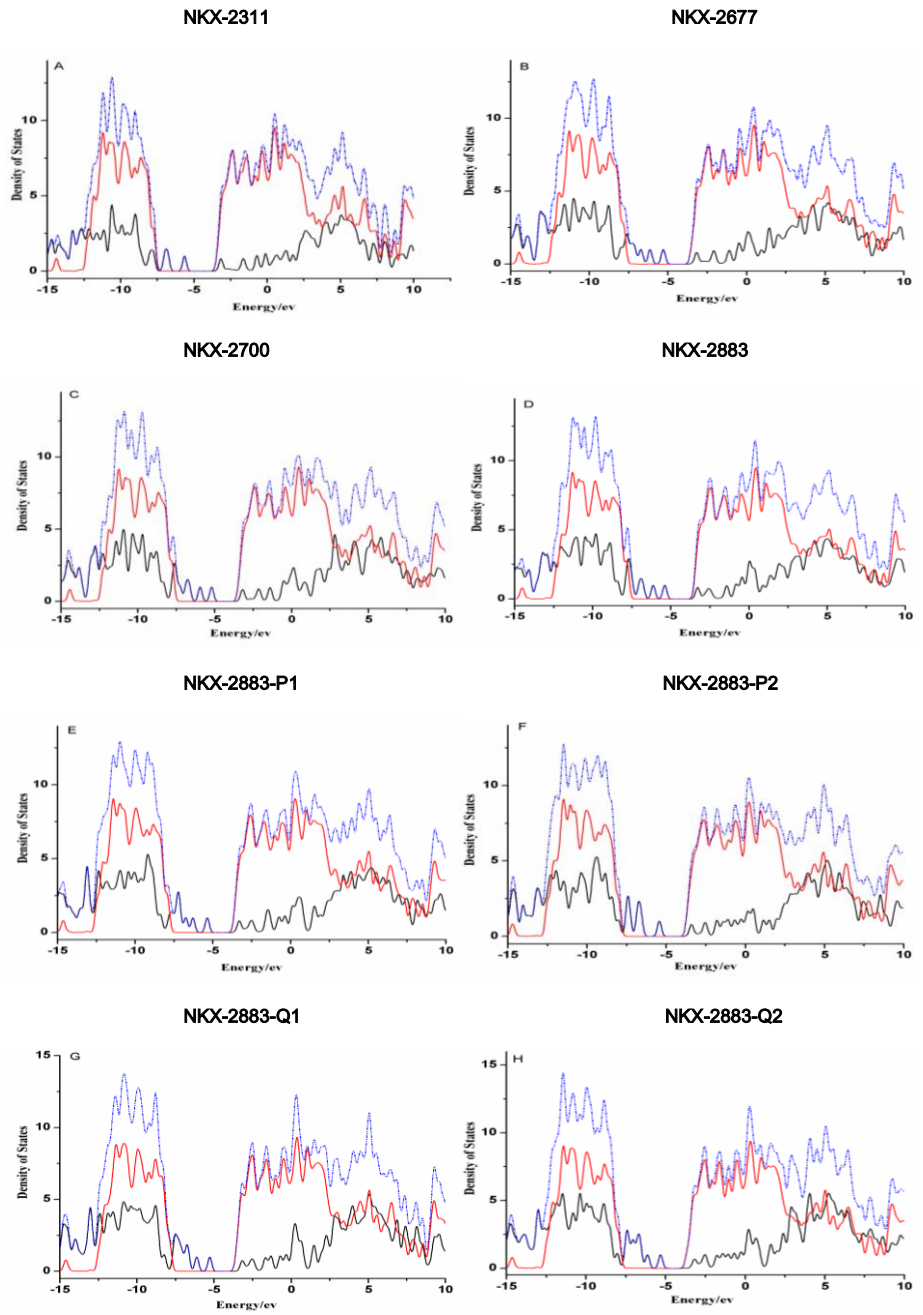

Fig. 4S Total densities of states (TDOS) and partial densities of states (PDOS) for the eight coumarin-based dyes (the blue dashed line corresponds to TDOS, the red full line corresponds to TiO_2 (PDOS), and the black line corresponds to dye (PDOS)).

NKX-2311	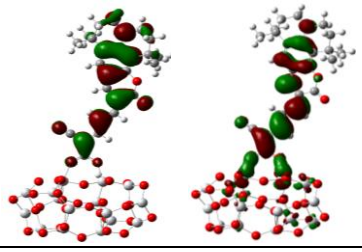					
	HOMO	LUMO				
NKX-2677	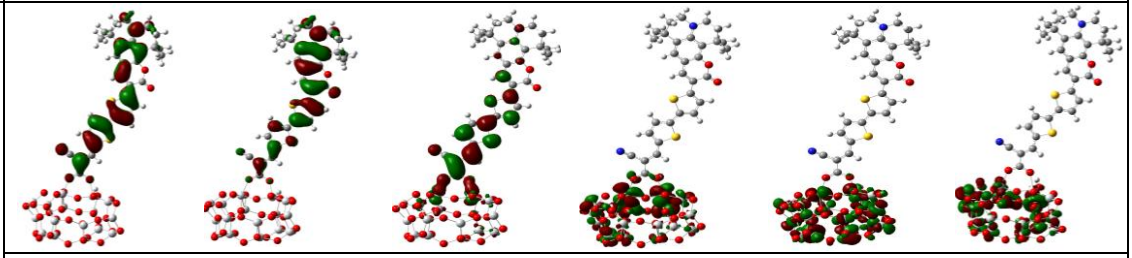					
	HOMO-1	HOMO	LUMO	LUMO+1	LUMO+8	LUMO+16
	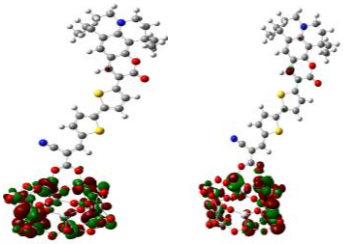					
	LUMO+17	LUMO+19				
NKX-2700	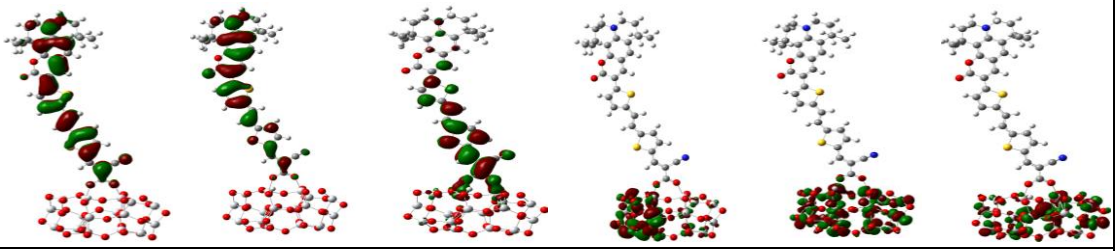					
	HOMO-1	HOMO	LUMO	LUMO+1	LUMO+8	LUMO+15
NKX-2883	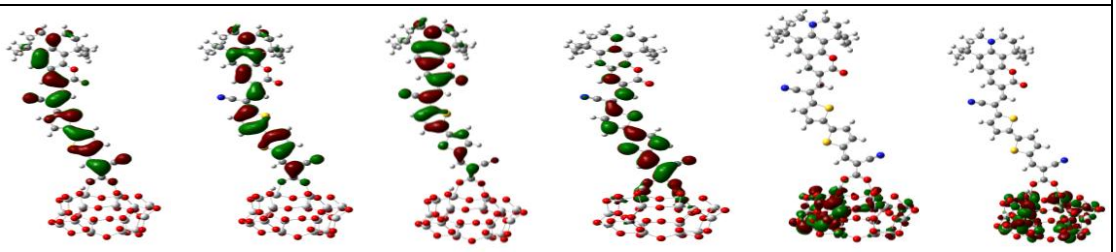					
	HOMO-3	HOMO-1	HOMO	LUMO	LUMO+3	LUMO+4
	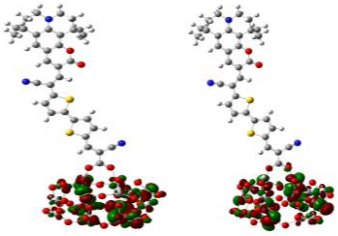					
	LUMO+5	LUMO+10				

NKX-2883-P1	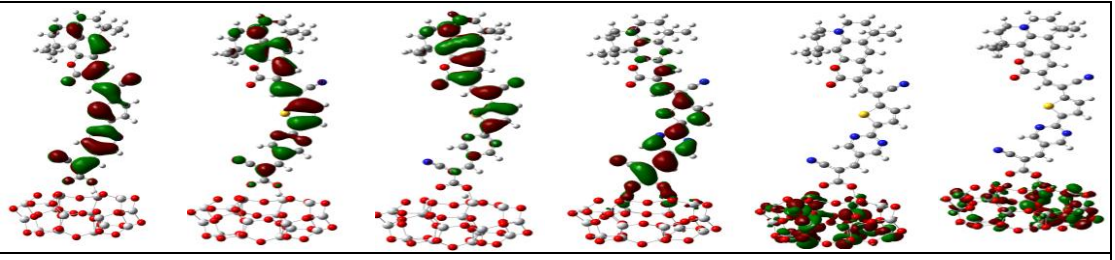					
	HOMO-3	HOMO-1	HOMO	LUMO	LUMO+2	LUMO+3
	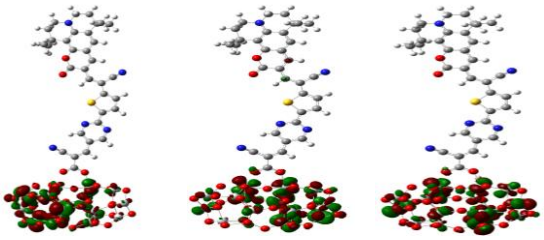					
	LUMO+5	LUMO+7	LUMO+10			
NKX-2883-P2	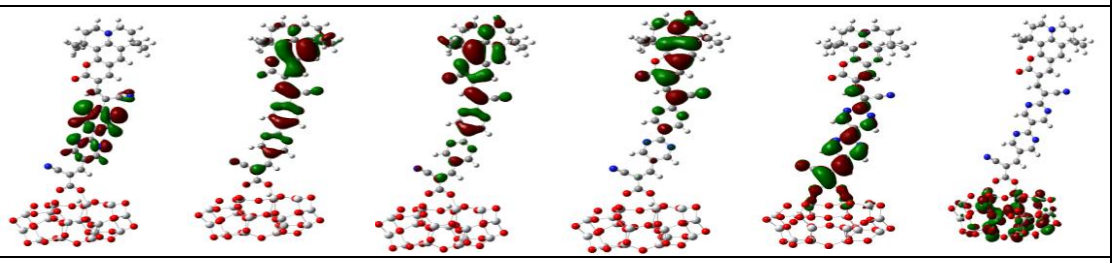					
	HOMO-3	HOMO-2	HOMO-1	HOMO	LUMO	LUMO+2
	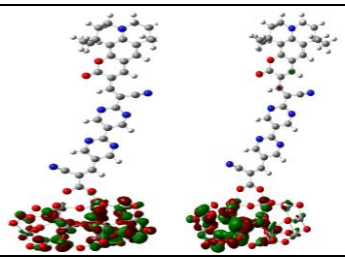					
	LUMO+3	LUMO+5				
NKX-2883-Q1	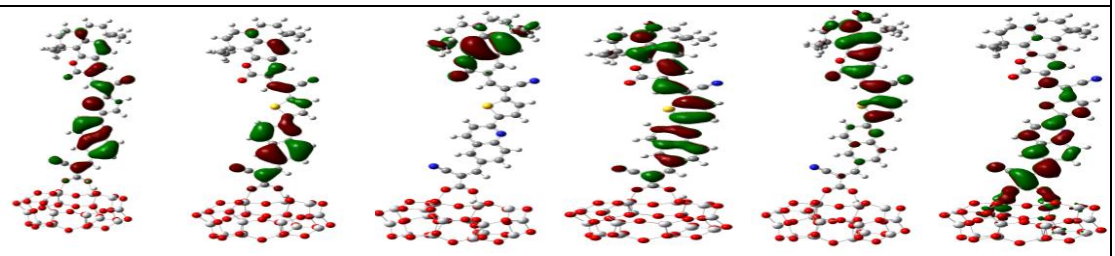					
	HOMO-4	HOMO-3	HOMO-2	HOMO-1	HOMO	LUMO
	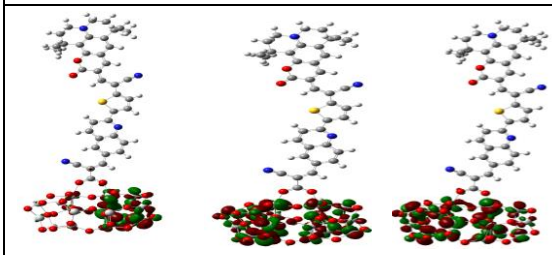					
	LUMO+3	LUMO+4	LUMO+5			

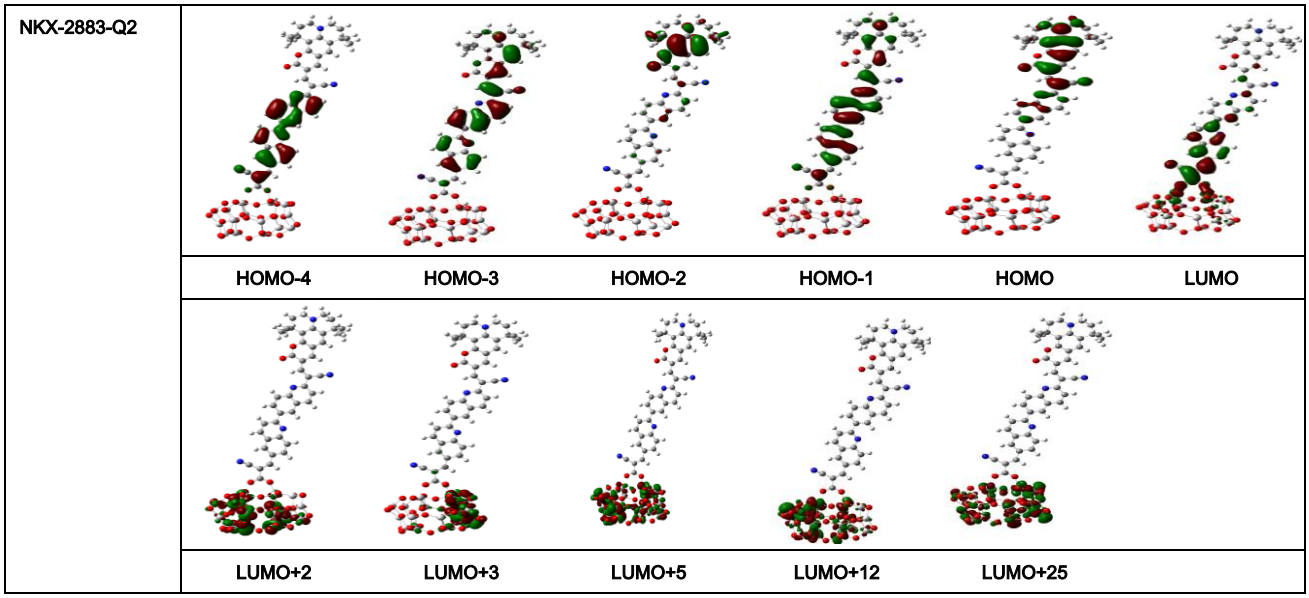

Fig. 5S Molecular orbitals relevant during photoexcitation for: 2311/TiO_2, 2677/TiO_2, 2700/TiO_2, 2883/TiO_2, 2883-P1/TiO_2, 2883-P2/TiO_2, 2883-Q1/TiO_2 and 2883-Q2/TiO_2 complexes (M062X)

NKX-2311	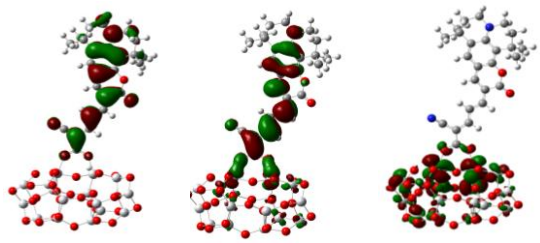					
	HOMO	LUMO	LUMO+3			
NKX-2677	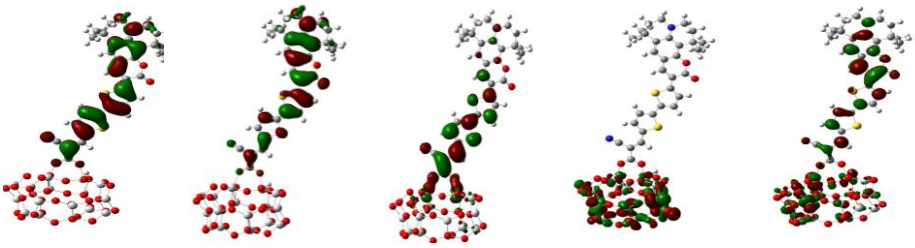					
	HOMO-1	HOMO	LUMO	LUMO+13	LUMO+23	
NKX-2700	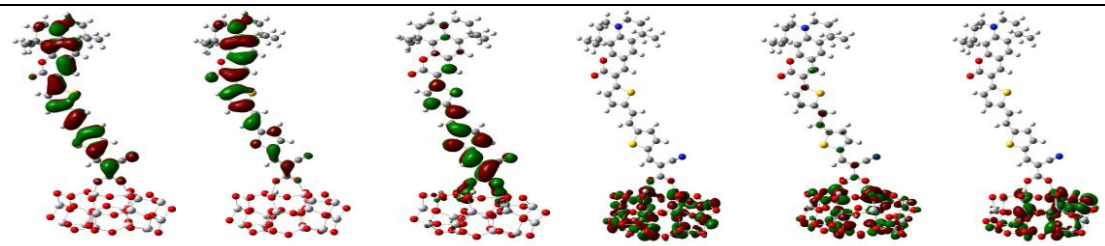					
	HOMO-1	HOMO	LUMO	LUMO+8	LUMO+9	LUMO+11
NKX-2883	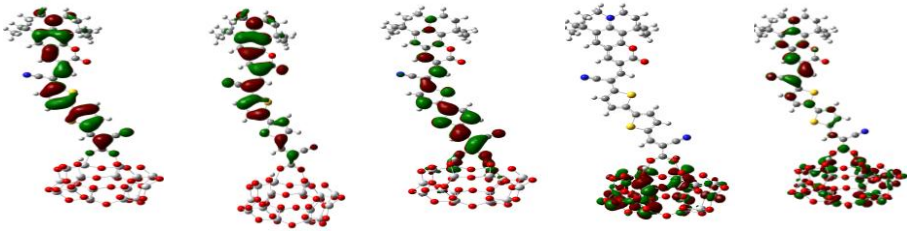					
	HOMO-1	HOMO	LUMO	LUMO+7	LUMO+8	
NKX-2883-P1	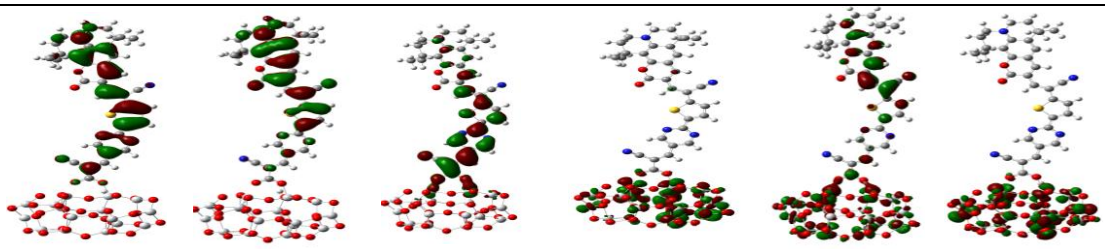					
	HOMO-1	HOMO	LUMO	LUMO+7	LUMO+8	LUMO+10
	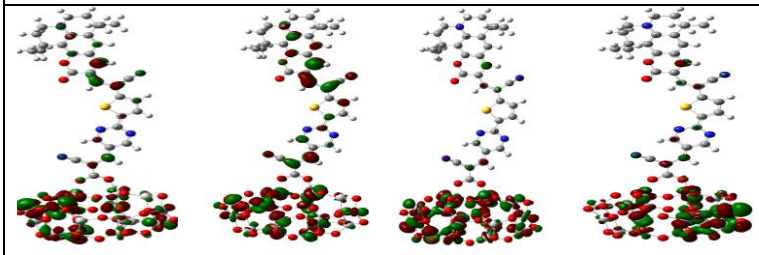					
	LUMO+11	LUMO+12	LUMO+13	LUMO+14		

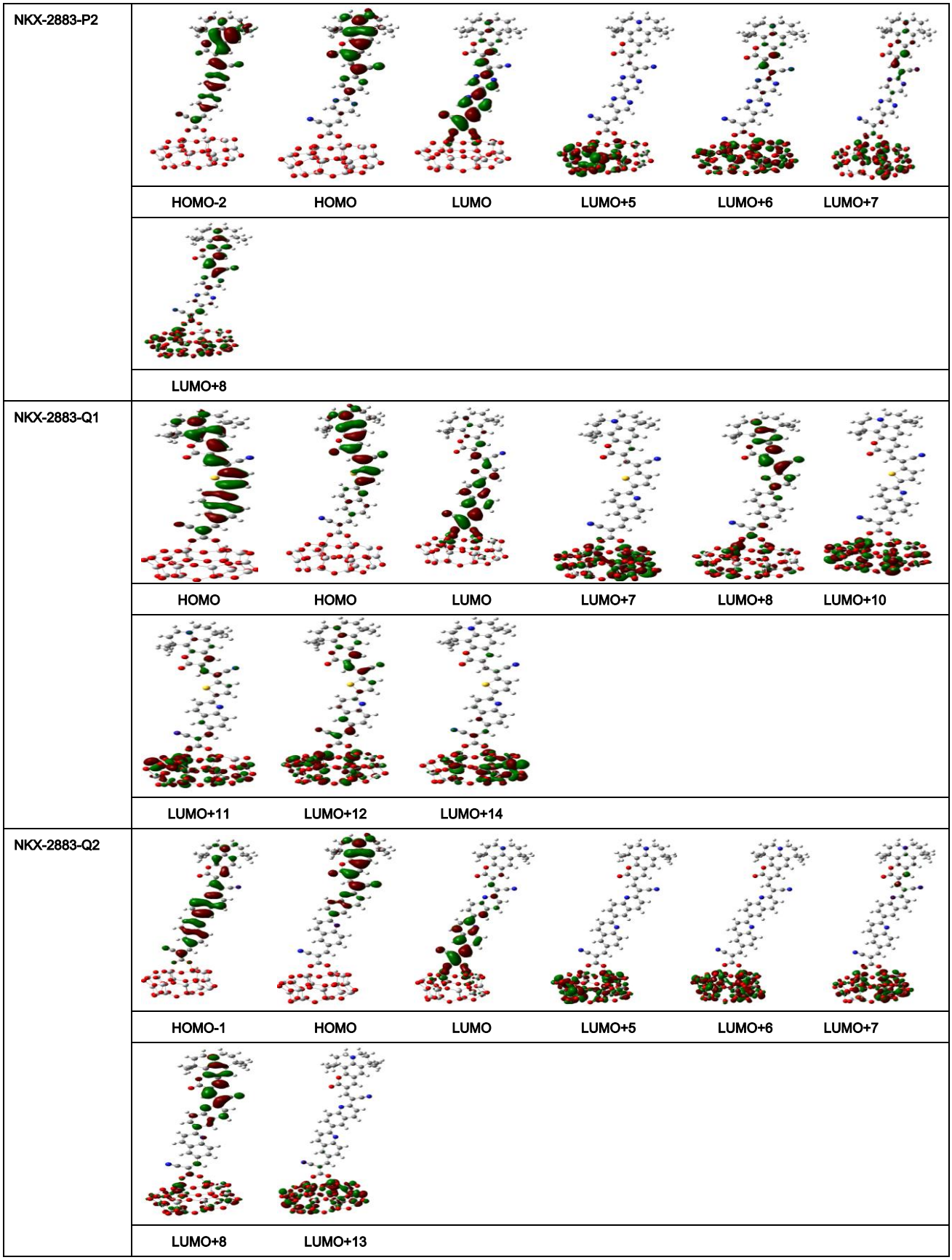

Fig. 6S Molecular orbitals relevant during photoexcitation for: 2311/TiO_2, 2677/TiO_2, 2700/TiO_2, 2883/TiO_2, 2883-P1/TiO_2, 2883-P2/TiO_2, 2883-Q1/TiO_2 and 2883-Q2/TiO_2. (B3LYP)

NKX-2311	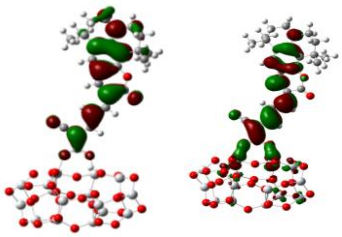					
	HOMO	LUMO				
NKX-2677	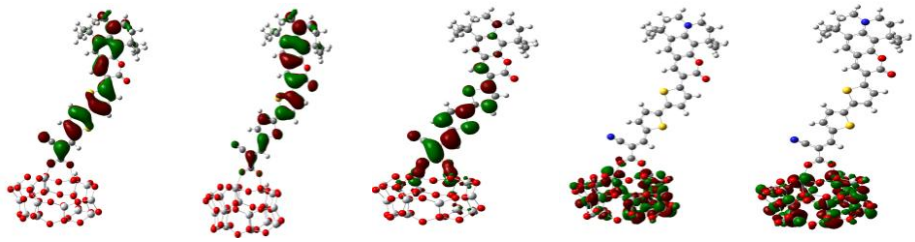					
	HOMO-1	HOMO	LUMO	LUMO+7	LUMO+8	
NKX-2700	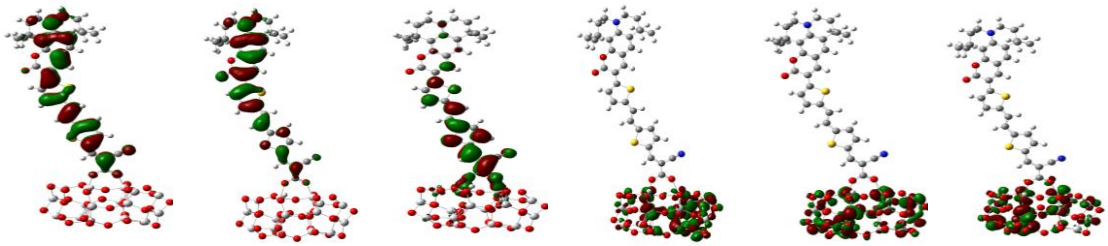					
	HOMO-1	HOMO	LUMO	LUMO+5	LUMO+6	LUMO+7
	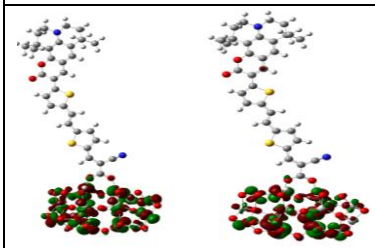					
	LUMO+8	LUMO+16				
NKX-2883	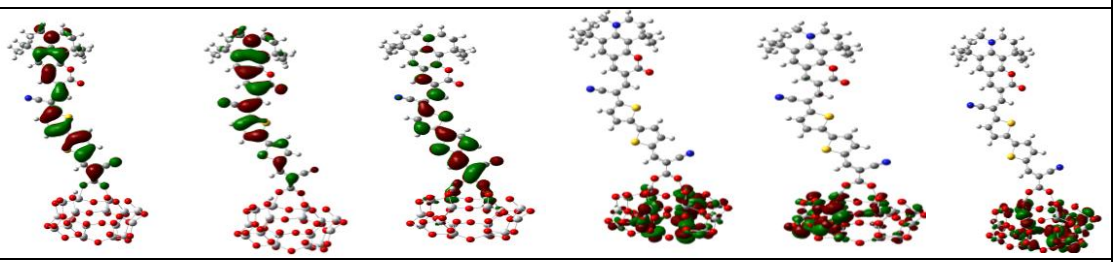					
	HOMO-1	HOMO	LUMO	LUMO+2	LUMO+3	LUMO+5
	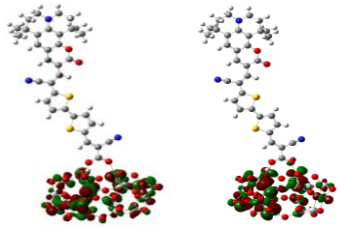					
	LUMO+6	LUMO+7				

NKX-2883-P1	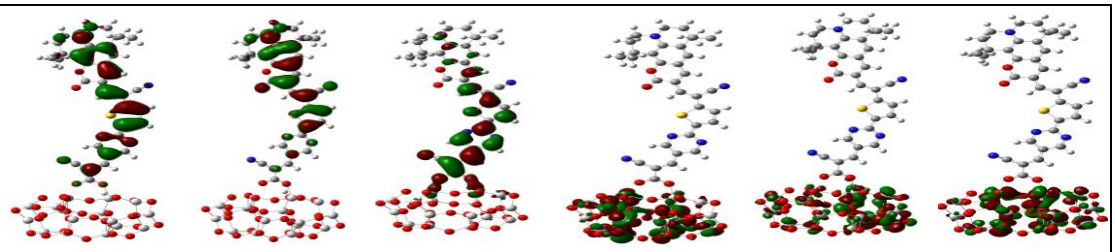					
	HOMO-1	HOMO	LUMO	LUMO+2	LUMO+3	LUMO+4
	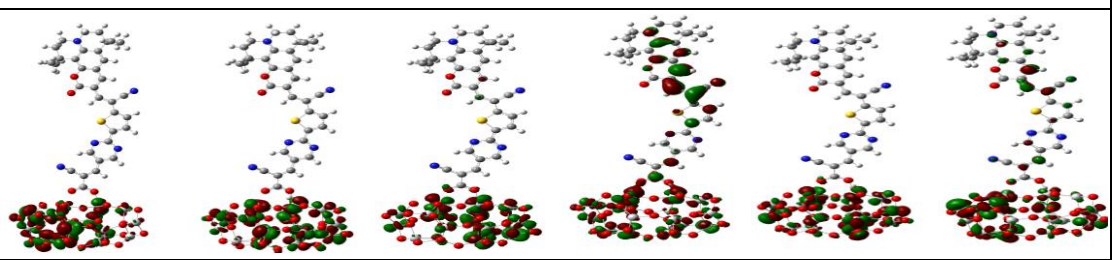					
	LUMO+5	LUMO+6	LUMO+7	LUMO+8	LUMO+10	LUMO+11
NKX-2883-P2	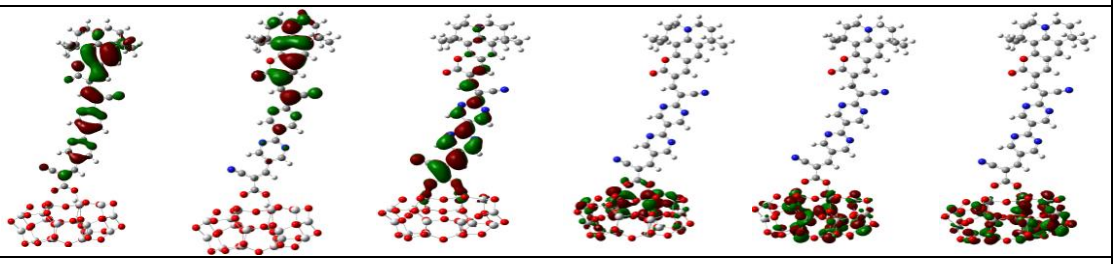					
	HOMO-2	HOMO	LUMO	LUMO+1	LUMO+2	LUMO+3
	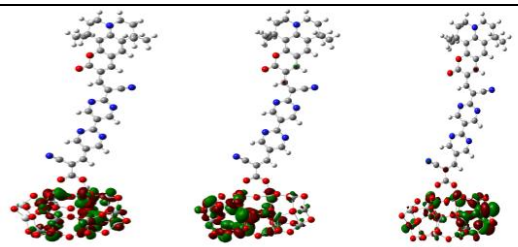					
	LUMO+4	LUMO+5	LUMO+13			
NKX-2883-Q1	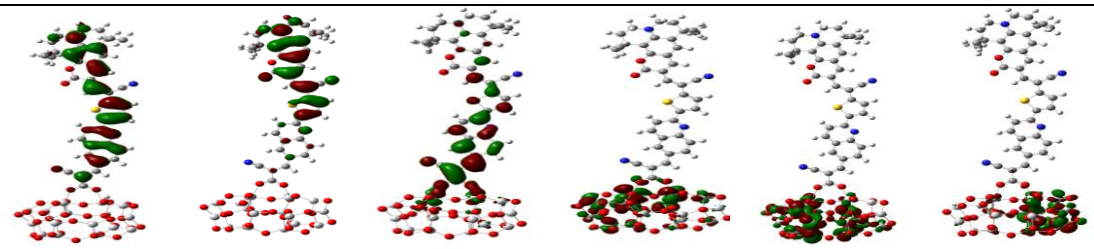					
	HOMO-1	HOMO	LUMO	LUMO+1	LUMO+2	LUMO+3
	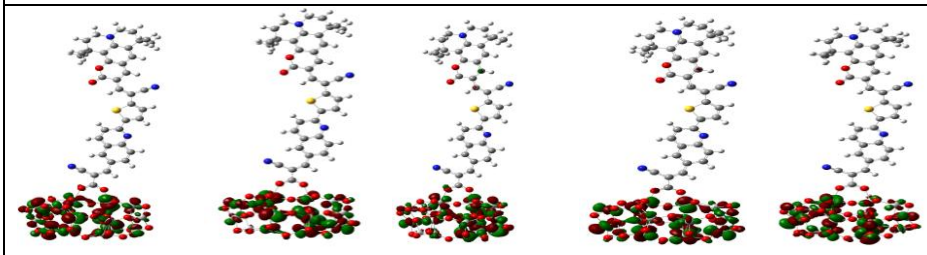					
	LUMO+5	LUMO+6	LUMO+7	LUMO+9	LUMO+10	

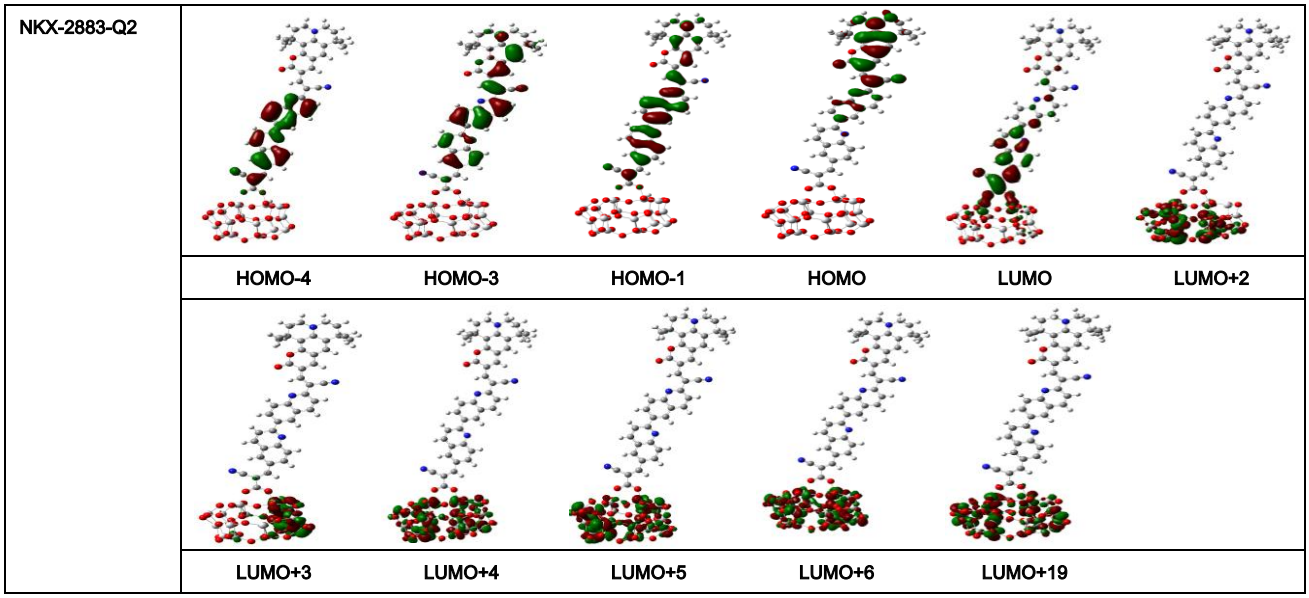

Fig. 7S Molecular orbitals relevant during photoexcitation for: 2311/TiO_2, 2677/TiO_2, 2700/TiO_2, 2883/TiO_2, 2883-P1/TiO_2, 2883-P2/TiO_2, 2883-Q1/TiO_2 and 2883-Q2/TiO_2 complexes. (PBE0)

	HOMO	HOMO-1	LUMO	LUMO+1
NKX-2311	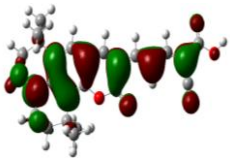	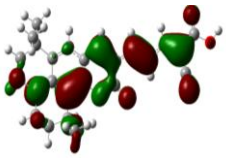	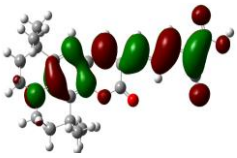	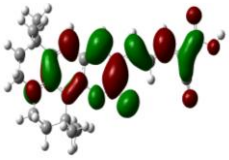
NKX-2677	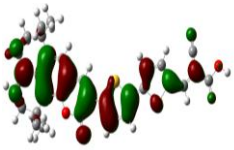	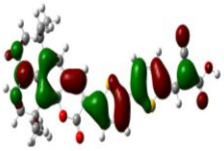	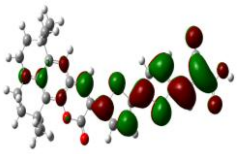	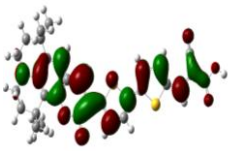
NKX-2677-P1	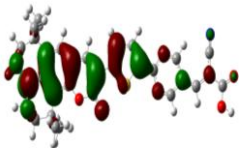	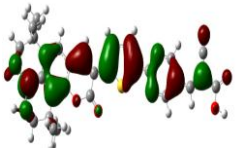	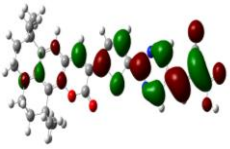	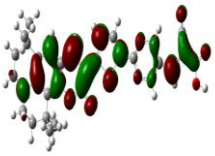
NKX-2677-P2	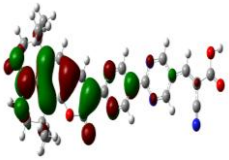	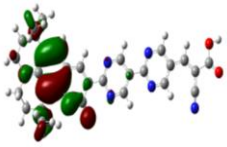	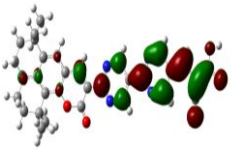	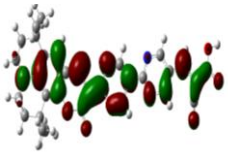
NKX-2700	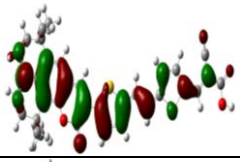	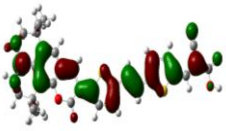	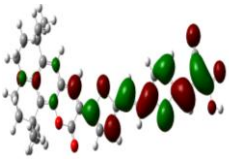	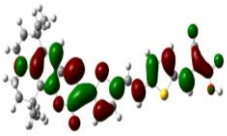
NKX-2700-P1	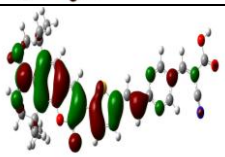		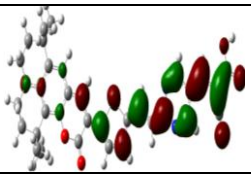	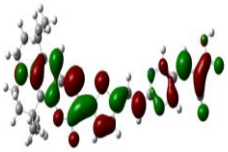
NKX-2700-P2	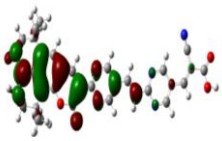		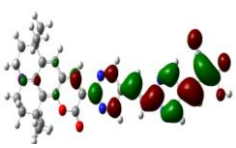	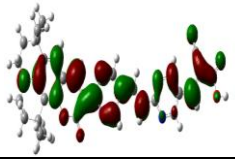
NKX-2883	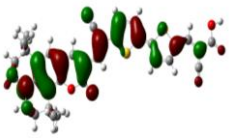	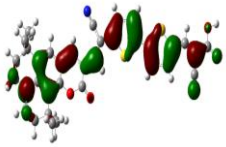	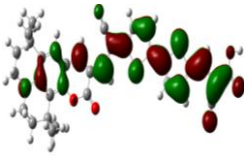	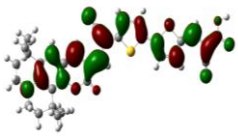
NKX-2883-P1	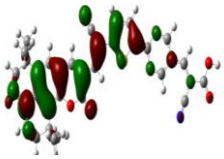	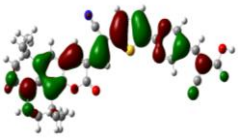	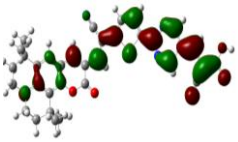	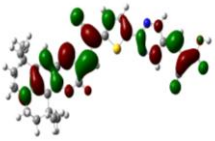
NKX-2883-P2	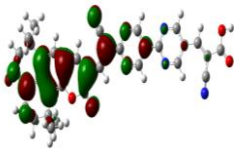	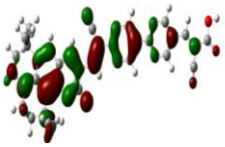	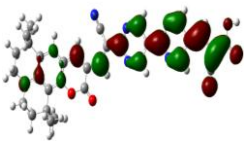	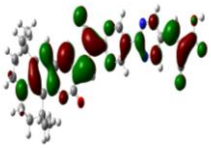

NKX-2883-Q1	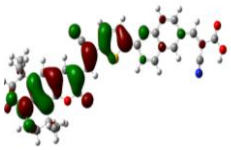	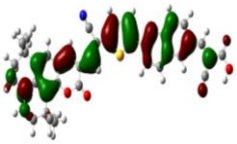	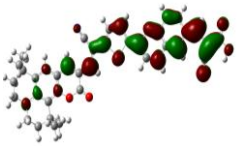	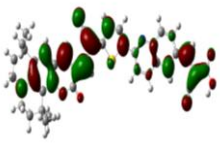
NKX-2883-Q2	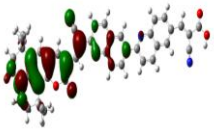	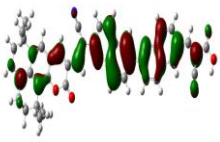	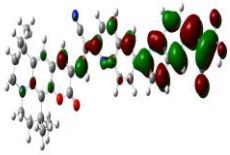	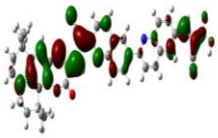

Fig. 8S Frontier molecular orbital spatial distribution for free dyes (B3LYP)

	HOMO	HOMO-1	LUMO	LUMO+1
NKX-2311	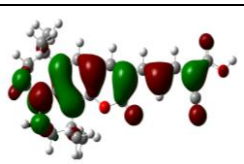	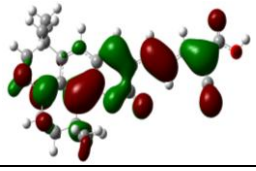	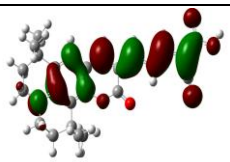	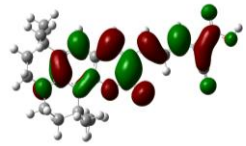
NKX-2677	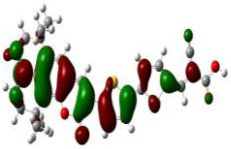		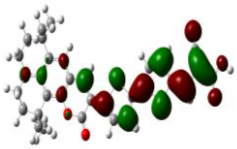	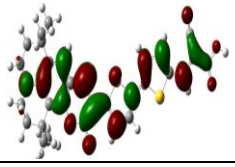
NKX-2677-P1	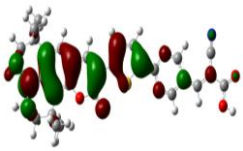	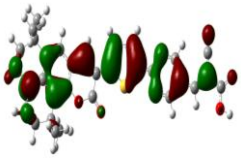	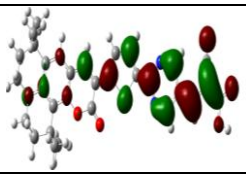	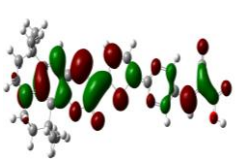
NKX-2677-P2	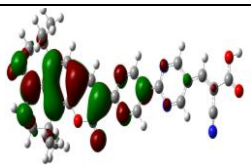	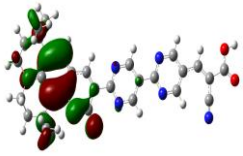	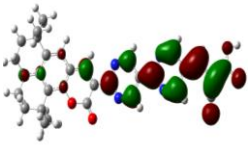	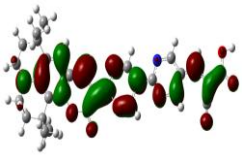
NKX-2700	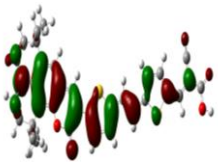	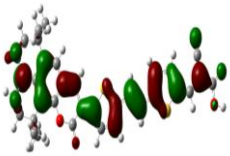	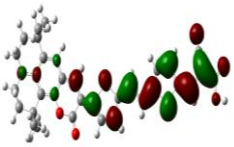	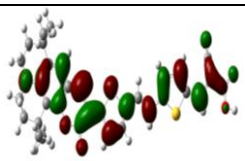
NKX-2700-P1	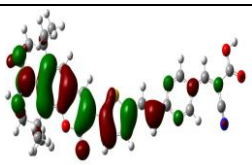	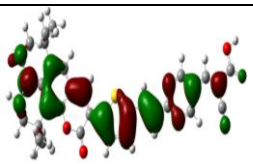	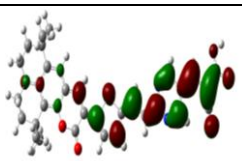	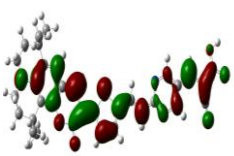
NKX-2700-P2	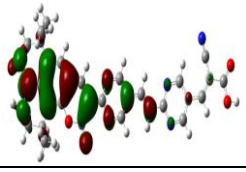	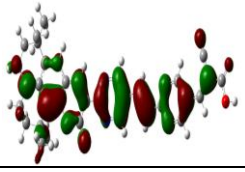	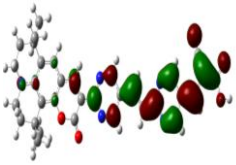	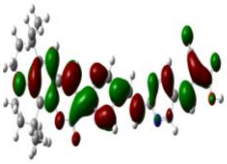
NKX-2883	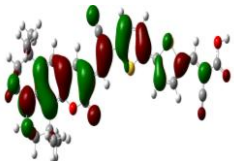	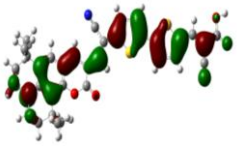	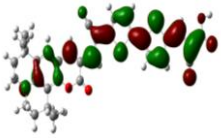	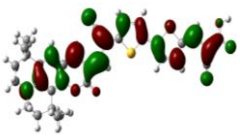
NKX-2883-P1	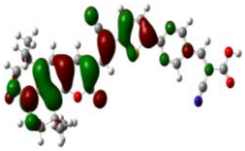	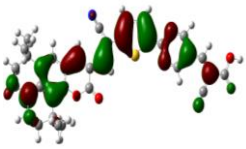	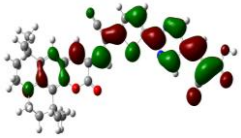	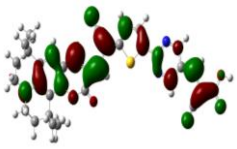
NKX-2883-P2	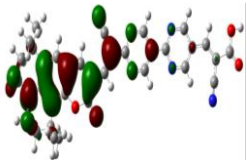	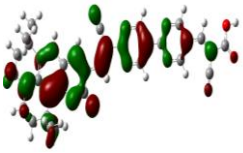	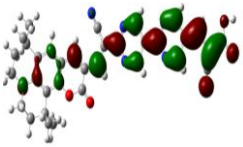	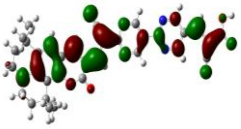

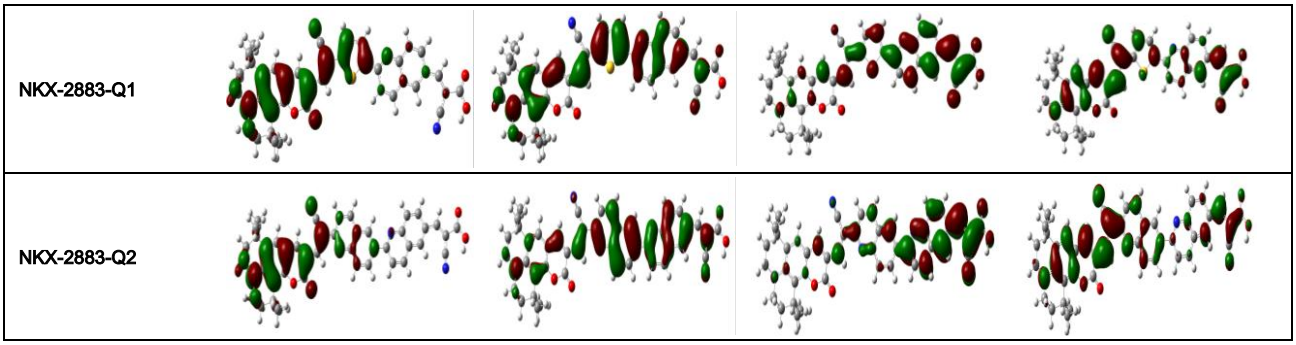

Fig. 9S Frontier molecular orbital spatial distribution for free dyes (PBE0)

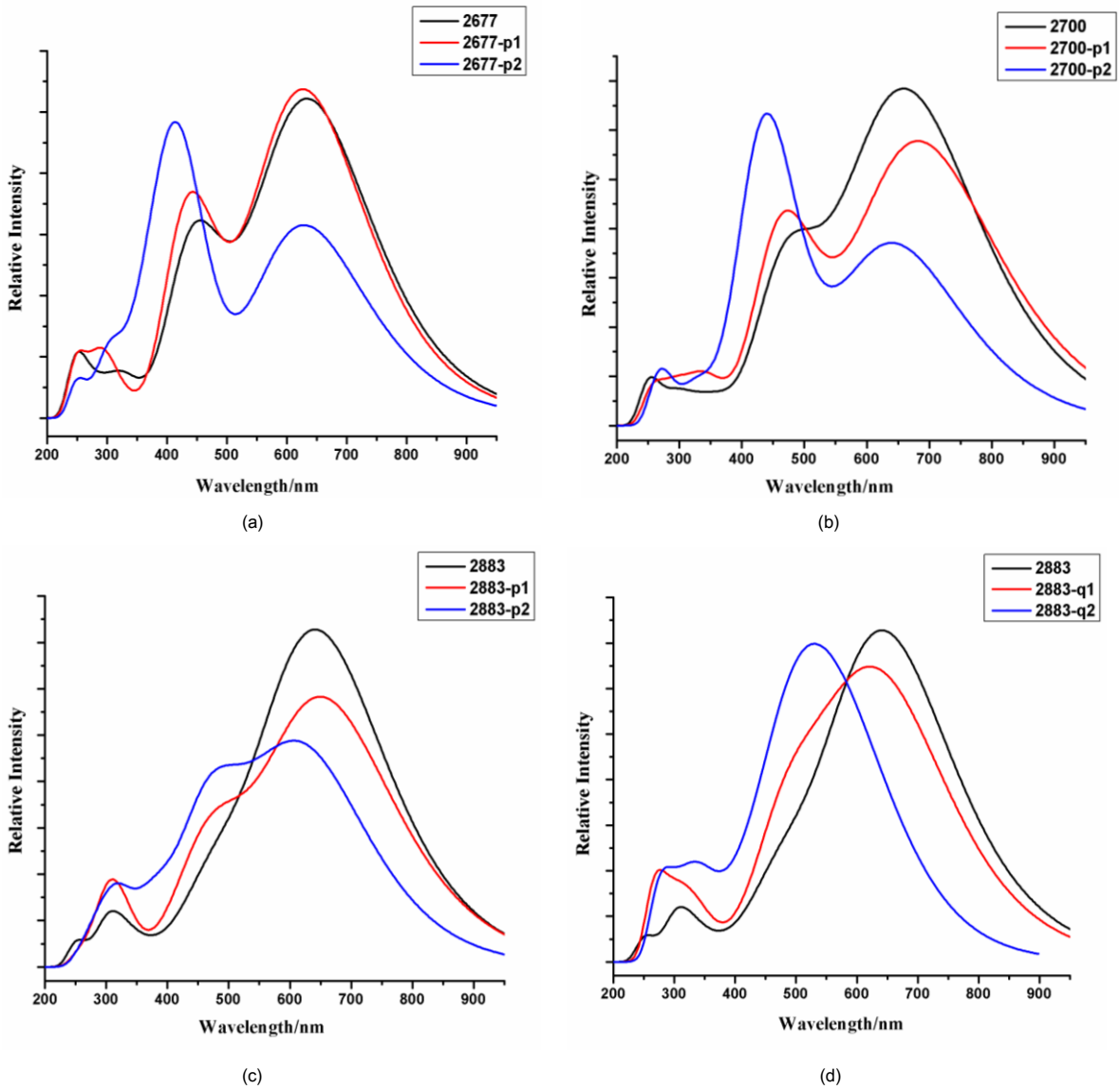

Fig. 10S Calculated UV/Vis absorption spectra four series sensitizers in ethanol solution obtained by B3LYP functional with 6-31G(d,p) basis set (a) NKX-2677, NKX-2677-P1 and NKX-2677-P2; (b) NKX-2700, NKX-2700-P1 and NKX-2700-P2; (c) NKX-2883, NKX-2883-P1 and NKX-2883-P2; (d) NKX-2883, NKX-2883-Q1 and NKX-2883-Q2

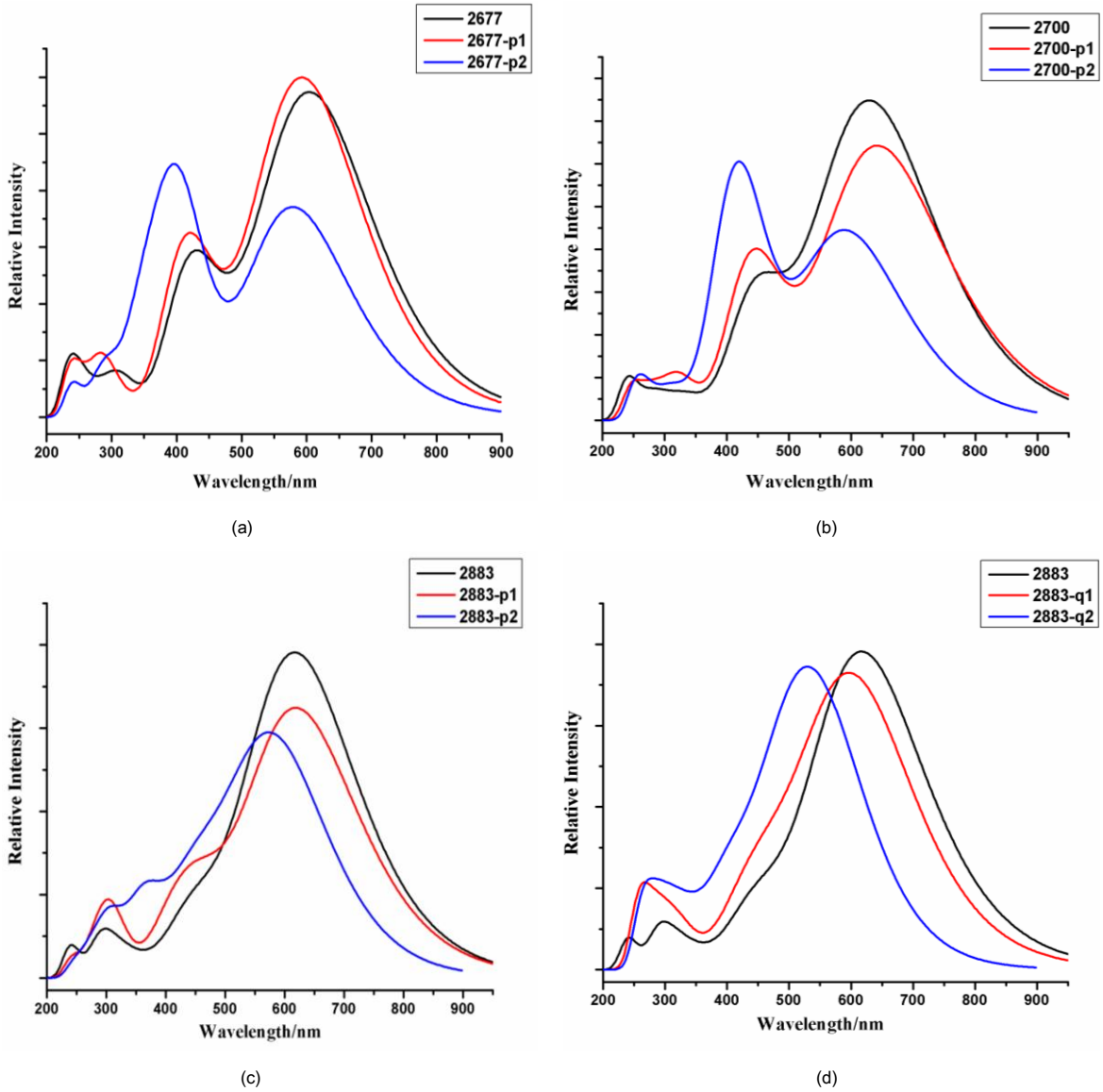

Fig. 11S Calculated UV/Vis absorption spectra four series sensitizers in ethanol solution obtained by B3LYP functional with 6-31G(d,p) basis set (a) NKX-2677, NKX-2677-P1 and NKX-2677-P2; (b) NKX-2700, NKX-2700-P1 and NKX-2700-P2; (c) NKX-2883, NKX-2883-P1 and NKX-2883-P2; (d) NKX-2883, NKX-2883-Q1 and NKX-2883-Q2

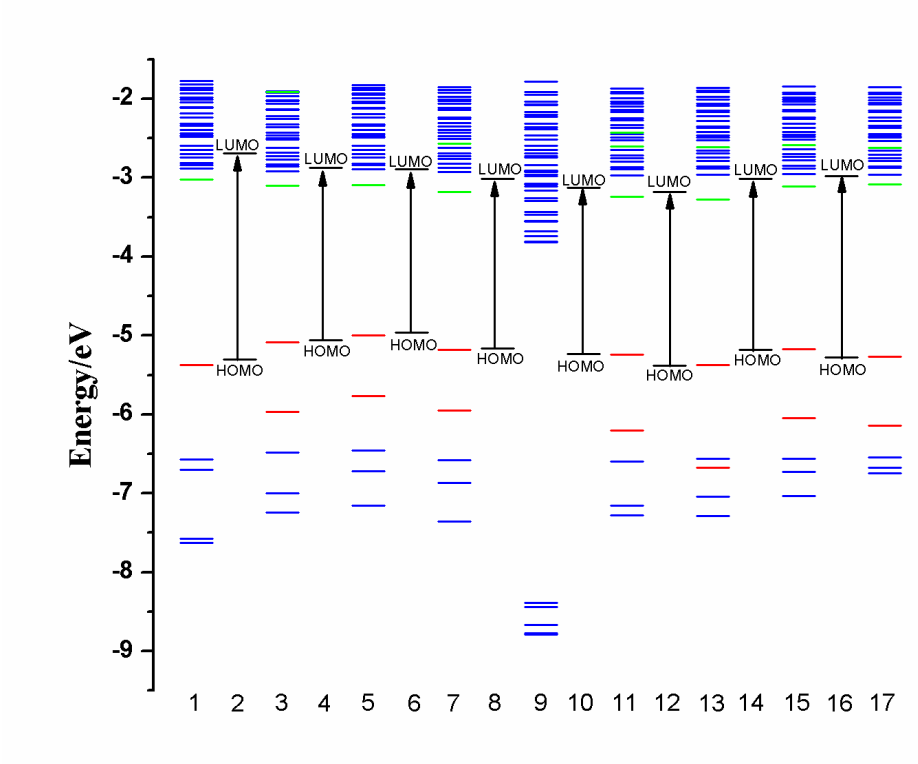

Fig. 12S Molecular orbital energy level (eV) diagram of (column 1) 2311/TiO_2 complex, (column 2) NKX-2311 dye, (column 3) 2677/TiO_2 complex, (column 4) NKX-2677 dye, (column 5) 2700/TiO_2 complex, (column 6) NKX-2700, (column 7) 2883/TiO_2 complex, (column 8) NKX-2883 dye, (column 9) isolated TiO_2, (column 10) NKX-2883-P1 dye, (column 11) 2883-P1/TiO_2 complex, (column 12) NKX-2883-P2 dye, (column 13) 2883-P2/TiO_2 complex, (column 14) NKX-2883-Q1 dye, (column 15) NKX-2883-Q1/TiO_2 complex, (column 16) NKX-2883-Q2 dye, (column 17) 2883-Q2/TiO_2 complex in ethanol solution. Green represents localization of molecular orbital both on the dye and the surface. Blue represents localization of molecular orbital on TiO_2. Red represents localization of molecular orbital on dyes (B3LYP)

Table 1S Transition energies (in eV) of S_0-S_1 transition for NKX-23111, NKX-2677, KNX-2700 and NKX-2883 coumarin dyes in ethanol solution with B3LYP/6-31g(d,p) geometries

Method	**2311**	**2677**	**2700**	**2883**	
B3LYP	2.468	1.946	1.864	1.909	ethanol
	2.479	1.966	1.879	1.922	THF
PBE0	2.528	2.047	1.962	1.998	
CAM-B3LYP	2.746	2.465	2.373	2.342	
LC-WPBE	2.916	2.759	2.682	2.598	
M062X	2.704	2.439	2.351	2.313	
WB97XD	2.779	2.549	2.550	2.407	
Experimental[a]	2.460	2.427	2.362	2.246	

a Experimental value from Ref. 12, 22, 23,24

Table 2S The HOMO energy levels (in eV) and corresponding oxidized potential (vs NHE, in eV) of ground state ($E_{ox(dye)}$) for NKX-2311, NKX-2677, NKX-2700, and NKX-2883. All values are calculated with B3LYP/6-31g(d,p) geometries

Method	**NKX-2311**		**NKX-2677**		**NKX-2700**		**NKX-2883**	
	HOMO	$E_{ox(dye)}$	**HOMO**	$E_{ox(dye)}$	**HOMO**	$E_{ox(dye)}$	**HOMO**	$E_{ox(dye)}$
B3LYP	5.307	0.867	4.967	0.527	5.055	0.615	5.161	0.721
PBE0	5.529	1.089	5.277	0.837	5.188	0.748	5.386	0.946
PBE0[a]	5.571	1.131	5.340	0.900	5.250	0.810	5.462	1.022
CAM-B3LYP	6.436	1.996	6.232	1.792	6.145	1.705	6.306	1.866
LC-WPBE	7.586	3.146	7.455	3.015	6.145	1.705	7.508	3.068
M062X	6.398	1.958	6.195	1.755	6.115	1.675	6.268	1.828
M062X[a]	6.444	2.004	6.194	1.754	6.091	1.651	6.300	1.860
WB97XD	7.003	2.563	6.813	2.373	6.740	2.300	6.879	2.439
Experimental[b]		1.3		0.91		0.82		0.97

a HOMO are computed by single point calculation based on the B3LYP/6-31g(d, p) optimized geometries.

b Experimental value from Ref. 12, 22, 23,24

Table 3S Transition energies (in eV) of S_0-S_1 transition for dyes (NKX-23111, NKX-2677, KNX-2700 and NKX-2883) in ethanol solution. Geometries structures are optimized with different functionals.

Method	**2311**	**2677**	**2700**	**2883**
B3LYP	2.468	1.946	1.864	1.909
PBE0	2.545	2.075	1.992	2.025
CAM-B3LYP	2.858	2.673	2.600	2.514
LC-WPBE	3.195	3.226	2.944	2.951
M062X	2.810	2.635	2.571	2.471
WB97XD	2.903	2.818	2.583	2.705
Experimental [a]	2.46	2.43	2.36	2.24

a Experimental value from Ref. 12, 22, 23,24

Table 4S Electronic transition data obtained by TD-M062X/6-31g(d,p) level for all free dyes and dye-titania complexes in ethanol solution with B3LYP/6-31g(d,p) geometries

Transition energy (eV)	Wavelength/ nm	Oscillator strength / Light harvesting efficiency	Wavelength
NKX-2311			
2.704($S_0 \rightarrow S_1$)	459	1.774/0.983	HOMO->LUMO (95%)
4.393($S_0 \rightarrow S_4$)	282	0.180/0.339	H-2->LUMO (28%), H-1->LUMO (48%), HOMO->L+1 (19%)
4.832($S_0 \rightarrow S_5$)	257	0.110/0.224	HOMO->L+2 (79%), H-2->LUMO (6%)
5.729($S_0 \rightarrow S_{12}$)	216	0.147/0.287	H-2->L+1 (75%), H-3->LUMO (8%)
6.397($S_0 \rightarrow S_{18}$)	194	0.314/0.517	H-2->L+2 (56%), HOMO->L+6 (14%)
6.483($S_0 \rightarrow S_{19}$)	191	0.101/0.207	H-10->LUMO (11%), H-8->LUMO (11%), H-1->L+2 (21%), HOMO->L+6 (15%),H-11->LUMO (7%), H-3->L+1 (8%), H-2->L+2 (6%),H-1
6.580($S_0 \rightarrow S_{20}$)	188	0.116/0.234	H-1->L+4 (18%), HOMO->L+4 (63%)
6.704($S_0 \rightarrow S_{22}$)	185	0.139/0.274	H-2->L+3 (38%), H-1->L+2 (25%), H-1->L+3 (17%), H-3->L+2 (5%)
7.055($S_0 \rightarrow S_{27}$)	176	0.102/0.209	H-10->LUMO (14%), H-3->L+1 (60%)
NKX-2311/TiO_2			
2.410($S_0 \rightarrow S_1$)	514	2.025/0.991	HOMO->LUMO (91%)
NKX-2677			
2.439($S_0 \rightarrow S_1$)	508	1.851/0.986	HOMO->LUMO (82%), H-1->LUMO (9%), HOMO->L+1 (6%)
3.329($S_0 \rightarrow S_2$)	372	0.177/0.334	H-1->LUMO (33%), HOMO->L+1 (61%)
3.640($S_0 \rightarrow S_3$)	341	0.180/0.339	H-1->LUMO (50%), HOMO->LUMO (14%), HOMO->L+1 (27%)
4.656($S_0 \rightarrow S_8$)	266	0.132/0.262	H-2->LUMO (10%), H-1->L+1 (19%), HOMO->L+2 (34%), HOMO->L+3 (16%),H-3->LUMO (6%)
6.057($S_0 \rightarrow S_{25}$)	205	0.112/0.227	H-13->LUMO (13%), H-5->L+1 (32%), H-6->L+1 (9%), H-5->L+2 (6%), H-3->L+2 (9%)
6.201($S_0 \rightarrow S_{27}$)	200	0.213/0.388	H-5->L+1 (10%), H-2->L+2 (14%), H-2->L+3 (29%), H-5->L+4 (5%)
6.230($S_0 \rightarrow S_{29}$)	199	0.320/0.521	H-13->LUMO (14%), H-6->L+1 (10%), H-5->L+1 (17%), H-2->L+3 (17%), H-5->L+2 (5%), H-2->L+2 (9%)
NKX-2677-TiO_2			
2.300($S_0 \rightarrow S_1$)	539	2.210/0.994	H-1->LUMO (11%), HOMO->LUMO (78%)
3.240($S_0 \rightarrow S_2$)	383	0.114/0.231	H-1->LUMO (36%), HOMO->L+16 (25%), HOMO->L+8 (5%), HOMO->L+17 (6%), HOMO->L+19 (7%)
3.480($S_0 \rightarrow S_4$)	356	0.231/0.413	H-1->LUMO (34%), HOMO->LUMO (15%), HOMO->L+1 (11%), HOMO->L+16 (11%)
NKX-2677-P1			
2.537($S_0 \rightarrow S_1$)	489	2.067/0.991	HOMO->LUMO (79%), HOMO->L+1 (11%),H-1->LUMO (7%)
3.819($S_0 \rightarrow S_3$)	325	0.277/0.472	H-1->LUMO (72%), HOMO->LUMO (12%),H-4->LUMO (5%), HOMO->L+1 (5%)
4.501($S_0 \rightarrow S_8$)	275	0.104/0.213	H-4->LUMO (14%), H-1->L+1 (28%), HOMO->L+3 (32%), H-2->LUMO (5%), HOMO->L+2 (5%), HOMO->L+4 (7%)
4.723($S_0 \rightarrow S_{10}$)	263	0.134/0.265	H-4->LUMO (12%), H-1->L+1 (30%), HOMO->L+3 (21%), HOMO->L+4 (16%), H-2->LUMO (9%)
6.205($S_0 \rightarrow S_{29}$)	200	0.175/0.332	H-14->LUMO (20%), H-4->L+1 (11%), H-2->L+4 (12%),

			H-1->L+2 (12%),H-15->LUMO (5%), H-2->L+3 (5%), H-1->L+3 (6%)
6.240(S_0→S_{30})	199	0.557/0.723	H-4->L+1 (10%), H-2->L+3 (19%), H-2->L+4 (43%)
NKX-2677-P2			
2.809(S_0→S_1)	441	1.789/0.984	HOMO->LUMO (70%), HOMO->L+1 (21%),H-2->LUMO (5%)
4.011(S_0→S_5)	309	0.678/0.790	H-4->LUMO (10%), H-2->LUMO (65%), H-1->LUMO (10%), HOMO->LUMO(9%)
6.153(S_0→S_{29})	202	0.446/0.642	H-1->L+3 (35%), H-1->L+5 (41%)
NKX-2700			
2.351(S_0→S_1)	527	2.350/0.996	HOMO->LUMO (81%),H-1->LUMO (9%), HOMO->L+1 (6%)
3.208(S_0→S_2)	387	0.170/0.324	H-1->LUMO (35%), HOMO->L+1 (56%)
3.516(S_0→S_3)	353	0.202/0.372	H-1->LUMO (46%), HOMO->LUMO (15%), HOMO->L+1 (29%)
5.847(S_0→S_{23})	212	0.117/0.236	H-8->LUMO (23%), H-6->L+1 (17%), H-5->L+1 (14%), H-3->L+2 (12%), H-4->L+1 (5%)
6.143(S_0→S_{28})	202	0.174/0.330	H-3->L+2(10%), H-2->L+2(17%), H-2->L+3(23%),H-1->L+3(11%), H-8->LUMO(6%), HOMO->L+5(6%), HOMO->L+10(5%)
6.200(S_0→S_{30})	200	0.325/0.527	H-2->L+2(10%), H-2->L+3(23%), H-1->L+3(23%),H-3->L+2(7%), H-3->L+3(8%), HOMO->L+5(7%), HOMO->L+6(5%)
NKX-2700/TiO2			
2.218(S_0→S_1)	559	2.710/0.998	H-1->LUMO (12%), HOMO->LUMO (77%)
3.115(S_0→S_2)	398	0.115/0.233	H-1->LUMO (41%), HOMO->L+15 (29%), HOMO->L+8 (5%)
3.369(S_0→S_3)	368	0.270/0.463	H-1->LUMO (32%), HOMO->LUMO (18%), HOMO->L+15 (18%), HOMO->L+1 (5%)
NKX-2700-P1			
2.403(S_0→S_1)	516	2.194/0.994	HOMO->LUMO (78%), HOMO->L+1 (11%),H-1->LUMO (9%)
3.327(S_0→S_2)	373	0.166/0.318	H-1->LUMO (18%), HOMO->L+1 (66%), HOMO->L+2 (8%)
3.594(S_0→S_3)	345	0.334/0.537	H-1->LUMO (60%), HOMO->LUMO (17%), HOMO->L+1 (12%)
4.543(S_0→S_{10})	273	0.132/0.259	H-4->LUMO (38%), H-3->LUMO (13%), HOMO->L+2 (10%), HOMO->L+3 (11%)
6.147(S_0→S_{30})	202	0.373/0.576	H-4->L+7 (15%), H-2->L+2 (27%), H-2->L+4 (36%), H-2->L+1 (7%)
NKX-2700-P2			
2.749(S_0→S_1)	451	2.178/0.993	H-1->LUMO (11%), HOMO->LUMO (64%), HOMO->L+1 (21%)
3.740(S_0→S_3)	331	0.578/0.736	H-1->LUMO (53%), HOMO->LUMO (27%), HOMO->L+1 (9%)
4.747(S_0→S_{11})	261	0.155/0.300	H-4->LUMO (13%), H-2->LUMO (13%), H-6->LUMO (8%), H-1->L+1 (13%),HOMO->L+3 (10%),HOMO->L+5 (21%), H-1->L+2 (5%)
NKX-2883			
2.313(S_0→S_1)	536	2.255/0.994	HOMO->LUMO (80%), H-1->LUMO (5%), HOMO->L+1 (9%)
3.053(S_0→S_2)	406	0.144/0.282	H-1->LUMO (32%), HOMO->L+1 (60%)
3.976(S_0→S_5)	312	0.105/0.215	H-2->LUMO (31%), H-2->L+1 (17%), H-1->L+1 (33%)
4.715(S_0→S_{10})	263	0.194/0.360	H-5->LUMO (13%), HOMO->L+3 (31%), HOMO->L+4 (18%), H-1->L+2 (9%), H-1->L+4 (5%)
6.040(S_0→S_{29})	205	0.337/0.540	H-2->L+2(40%),H-2->L+3(29%)，H-2->L+1 (7%), HOMO->L+8 (5%)
NKX-2883/TiO_2			
2.230(S_0→S_1)	556	2.627/0.998	HOMO->LUMO (74%), H-1->LUMO (8%), HOMO->L+3 (5%)

2.951($S_0 \rightarrow S_2$)	420	0.103/0.211	H-1->LUMO (29%), HOMO->L+3 (17%), HOMO->L+5 (20%), HOMO->L+4 (5%), HOMO->L+7 (7%), HOMO->L+10 (7%)
3.383($S_0 \rightarrow S_3$)	366	0.174/0.330	H-1->LUMO (51%), HOMO->LUMO (18%), HOMO->L+3 (6%), HOMO->L+5 (6%)
3.897($S_0 \rightarrow S_8$)	318	0.102/0.209	H-3->LUMO (11%), H-1->L+3 (11%), H-1->L+5 (21%), HOMO->L+5 (10%), H-1->L+7 (6%), HOMO->L+3 (6%)
NKX-2883-P1			
2.356($S_0 \rightarrow S_1$)	526	2.001/0.990	HOMO->LUMO(76%),HOMO->L+1(16%),H-1->LUMO (5%
3.212($S_0 \rightarrow S_2$)	386	0.203/0.373	H-1->LUMO (16%), HOMO->L+1(68%), HOMO->LUMO (7%)
3.629($S_0 \rightarrow S_3$)	342	0.206/0.378	H-1->LUMO (68%), HOMO->LUMO (12%), HOMO->L+1(9%)
4.156($S_0 \rightarrow S_6$)	298	0.295/0.493	H-3->LUMO (21%), H-1->L+1(46%), HOMO->L+2(16%)
NKX-2883-P1/TiO_2			
2.322($S_0 \rightarrow S_1$)	534	2.237/0.994	HOMO->LUMO (70%), H-1->LUMO (6%), HOMO->L+3(6%), HOMO->L+5(8%)
3.131($S_0 \rightarrow S_2$)	396	0.226/0.406	H-1->LUMO (14%), HOMO->LUMO (10%), HOMO->L+3(15%), HOMO->L+5(26%), HOMO->L+2(5%), HOMO->L+7(6%), HOMO->L+10(7%)
3.545($S_0 \rightarrow S_3$)	350	0.341/0.544	H-1->LUMO (64%), HOMO->LUMO (16%), H-3->LUMO (5%)
4.077($S_0 \rightarrow S_{10}$)	304	0.105/0.215	HOMO->L+5 (31%), HOMO->L+7 (25%),H-3->LUMO (6%), H-1->L+5 (8%)
4.101($S_0 \rightarrow S_{11}$)	302	0.161/0.310	H-3->LUMO (11%), H-1->L+5(10%), HOMO->L+7(35%), H-1->L+3(7%)，H-1->L+7(5%)
NKX-2883-P2			
2.530($S_0 \rightarrow S_1$)	490	2.024/0.991	HOMO->LUMO (63%), HOMO->L+1 (30%)
3.894($S_0 \rightarrow S_4$)	318	0.242/0.427	H-2->L+1(19%), H-1-> LUMO (53%),H-3->LUMO (5%), H-1->L+1 (7%), HOMO->LUMO (5%)
3.933($S_0 \rightarrow S_5$)	315	0.376/0.579	H-2->LUMO (44%), H-2->L+1 (18%), H-1->LUMO (11%), H-3->LUMO (5%), HOMO->LUMO (6%)
4.339($S_0 \rightarrow S_7$)	286	0.240/0.425	H-3->LUMO (21%), H-1->L+1 (25%), HOMO->L+3 (31%), HOMO->L+5 (9%)
NKX-2883-P2/TiO_2			
2.514($S_0 \rightarrow S_1$)	493	2.218/0.994	HOMO->LUMO (56%), HOMO->L+3 (17%), HOMO->L+2 (9%), HOMO->L+5 (8%)
3.819($S_0 \rightarrow S_4$)	325	0.793/0.839	H-3->LUMO (14%), H-1->LUMO (52%), HOMO->LUMO (12%), H-2->LUMO (7%)
NKX-2883-Q1			
2.432($S_0 \rightarrow S_1$)	510	2.270/0.995	HOMO->LUMO (64%), HOMO->L+1 (27%)
3.177($S_0 \rightarrow S_2$)	390	0.199/0.368	H-1->LUMO (24%), HOMO->LUMO (11%), HOMO->L+1 (53%)
3.623($S_0 \rightarrow S_3$)	342	0.227/0.407	H-1->LUMO (54%), HOMO->LUMO (17%), HOMO->L+1 (11%), H-3->LUMO (5%)
4.019($S_0 \rightarrow S_6$)	308	0.171/0.325	H-4->LUMO (24%),H-1->L+1(42%),H-2->LUMO (6%), HOMO->L+3 (9%)
4.718($S_0 \rightarrow S_{12}$)	262	0.220/0.397	H-1->L+3 (10%), HOMO->L+4 (24%), HOMO->L+5 (21%),

			H-5->LUMO (7%), H-3->L+1 (5%), HOMO->L+3 (8%)
5.049(S_0→S_{15})	246	0.295/0.493	H-3->L+2 (27%), HOMO->L+5 (17%), HOMO->L+4 (6%)
5.388(S_0→S_{22})	230	0.133/0.264	H-5->L+1(33%), H-1->L+2(12%), H-5->LUMO (6%), H-4->L+1 (6%), H-4->L+2 (6%), H-3->L+2 (8%
NKX-2883-Q1/TiO_2			
2.4194(S_0→S_1)	512	2.510/0.997	HOMO->LUMO (56%), HOMO->L+3 (11%), HOMO->L+5 (11%), H-1->LUMO (5%)
3.1208(S_0→S_2)	397	0.270/0.463	H-1->LUMO (23%), HOMO->LUMO (15%), HOMO->L+3 (12%), HOMO->L+5(19%), HOMO->L+4 (6%)
3.564(S_0→S_3)	348	0.364/0.567	H-1->LUMO (47%), HOMO->LUMO (23%), H-3->LUMO (7%)
3.989(S_0→S_9)	311	0.124/0.248	H-4->LUMO (13%), H-2->LUMO (15%), H-1->L+5 (10%), H-2->L+3 (7%)), H-2->L+5 (9%), H-1->L+3 (7%)
NKX-2883-Q2			
2.602(S_0→S_1)	476	2.117/0.992	HOMO->LUMO (37%), HOMO->L+1 (55%)
3.359(S_0→S_2)	369	0.607/0.753	H-1->LUMO (44%), HOMO->LUMO (18%), HOMO->L+1 (22%)
3.723(S_0→S_3)	333	0.226/0.406	H-3->LUMO (10%), H-1->LUMO (27%), HOMO->LUMO (36%), HOMO->L+1 (13%)
4.077(S_0→S_7)	304	0.102/0.209	H-5->LUMO (14%), H-4->LUMO (29%), H-1->L+1 (22%), H-4->L+2 (5%)
4.554(S_0→S_{11})	272	0.149/0.290	H-1->L+2(18%), HOMO->L+5(23%),H-5->L+1 (5%),, H-3->L+1 (7%), H-2->L+1 (8%),, HOMO->L+4 (5%)
4.813(S_0→S_{14})	258	0.201/0.370	H-1->L+2 (12%), HOMO->L+5 (11%), HOMO->L+6 (25%), H-3->L+1 (5%), HOMO->L+3 (7%)
4.898(S_0→S_{16})	253	0.175/0.332	H-4->LUMO (15%), H-4->L+1 (10%), HOMO->L+4 (27%), HOMO->L+6 (10%),H-3->LUMO (7%, H-1->L+4 (8%)
5.069(S_0→S_{18})	245	0.448/0.644	H-3->L+2(10%), HOMO->L+3(10%), H-6->L+1 (6%), H-5->LUMO (6%), H-5->L+1 (8%), H-5->L+2 (5%), H-4->L+2 (5%), H-3->L+3 (7%)
5.419(S_0→S_{25})	229	0.253/0.442	H-3->L+1 (14%), H-6->LUMO (9%), H-5->L+2 (5%), H-5->L+3 (7%), H-4->L+3 (6%), H-1->L+2 (5%), HOMO->L+4 (5%)
5.577(S_0→S_{29})	222	0.256/0.445	H-4->L+2 (21%), H-6->L+1 (5%), H-4->L+3 (5%), H-1->L+3 (5%)
NKX-2883-Q2/TiO_2			
2.592(S_0→S_1)	478	2.332/0.995	HOMO->LUMO (27%), HOMO->L+2 (20%), HOMO->L+3 (32%), HOMO->L+5 (6%)
3.270(S_0→S_2)	379	0.794/0.839	H-1->LUMO (44%), HOMO->LUMO (20%), HOMO->L+3 (9%)
3.637(S_0→S_3)	341	0.331/0.533	H-1->LUMO (25%), HOMO->LUMO (46%), H-3->LUMO (6%)
4.045(S_0→S_8)	307	0.113/0.229	H-4->LUMO(26%), H-1->L+3(11%), H-5->LUMO (9%), H-1->L+2 (6%)
4.531(S_0→S_{26})	274	0.130/0.259	H-1->L+25 (14%), HOMO->L+56 (12%), HOMO->L+12 (5%)

Table 5S Estimated $\Delta G_{(aq)}$, ΔG^0 , ΔE_{ver}, $E_{ox(dye)}$, ΔG_{reg}, f and LHE for all coumarin sensitizers. All calculation is obtained by M062X functional with b-31g(d,p) basis set

scheme	$\Delta G(aq)$ [a]	ΔG^0 [b]	E_{redox} [c]	ΔE_{ver} [d]	$E_{ox(dye)}$ [e]	$E_{ox(dye^*)}$ [f]	ΔG_{reg} [g]	f [h]	LHE [i]
NKX-2311	10.501	-2.917	6.061	2.704	-2.004	-0.700	-1.704	1.774/ 0.314	0.983/0.514
NKX-2677	9.401	-2.083	4.961	2.439	-1.754	-0.685	-1.454	1.851/ 0.320	0.986/0.521
NKX-2677-P1	9.720	-2.303	5.278	2.537	-1.804	-0.733	-1.504	2.067/ 0.557	0.991/0.723
NKX-2677-P2	10.468	-2.779	6.028	2.81	-1.945	-0.864	-1.645	1.789/ 0.678	0.984/0.790
NKX-2700	9.078	-1.847	4.638	2.351	-1.651	-0.700	-1.351	2.347/ 0.325	0.996/0.527
NKX-2700-P1	9.464	-2.182	5.024	2.403	-1.724	-0.679	-1.424	2.194/ 0.373	0.994/0.576
NKX-2700-P2	10.093	-2.464	5.653	2.750	-1.918	-0.831	-1.618	2.178/ 0.578	0.993/0.736
NKX-2883	9.265	-2.072	4.825	2.313	-1.860	-0.454	-1.560	2.255/ 0.337	0.994/0.540
NKX-2883-P1	9.589	-2.353	5.149	2.356	-1.876	-0.480	-1.576	2.001/0.295	0.990/0.493
NKX-2883-P2	10.267	-2.856	5.827	2.530	-2.006	-0.524	-1.706	2.024/0.376	0.991/0.579
NKX-2883-Q1	9.385	-2.073	4.945	2.432	-1.888	-0.544	-1.588	2.270/ 0.295	0.995/0.493
NKX-2883-Q2	9.627	-2.145	5.187	2.602	-1.956	-0.646	-1.656	2.117/ 0.607	0.992/0.753

[a]Calculated Gibbs free energy change ($\Delta G_{(aq)}$, in V) due to the oxidation of the dyes in aqueous solutions. [b]The driving force(ΔG^0, in V) electron injection related to the electronic transition in B1 band. [c]Redox potential (E_{redox} vs NHE, in V). [d] The vertical excitation energy (ΔE_{ver}, eV) corresponding to the maximum wavelength of spectral absorption. [e]The oxidized potential (vs. NHE, $E_{ox(dye)}$, in eV) of ground state. [f]The oxidized potential of the first excited state ($E_{ox(dye^*)}$) following unrelax path for dyes.[g]The regeneration energy(ΔG_{reg} , in V). [h] The oscillation strength of the two major absorption bands (B1 and B2 bands).[i]The light harvest efficiency (LHE) corresponding to B1/B2 bands.

Table 6S Maximum absorption wavelength (λ_{max}) and corresponding oscillation strength (f) and light harvesting efficiency (φ_{LHE}) for NKX-2311, NKX-2677, NKX-2700, and NKX-2883

Molecule	NKX-2311(Exp)	NKX-2677(Exp)	NKX-2700(Exp)	NKX-2883(Exp)
λ_{max}	2.704(2.460) [a]	2.439(2.427) [a]	2.351(2.362) [a]	2.313(2.246)[a]
f	1.774	1.851	2.347	2.255
φ_{LHE}	0.983	0.986	0.996	0.994

a Experimental value from Ref. 12, 22, 23, 24

Table 7S Estimated $\Delta G_{(aq)}$, ΔG^0 , ΔE_{ver}, $E_{ox(dye)}$, ΔG_{reg}, f and LHE for all coumarin sensitizers. All calculation is obtained by B3LYP functional with b-31g(d,p) basis set

scheme	$\Delta G(aq)$ [a]	ΔG^{0} [b]	E_{redox} [c]	ΔE_{ver} [d]	$E_{ox(dye)}$ [e]	$E_{ox(dye^*)}$ [f]	ΔG_{reg} [g]	f [h]	LHE [i]
NKX-2311	6.324	-1.024	1.884	2.468	-0.867	-1.601	-0.567	1.553/ 0.504	0.972/0.687
NKX-2677	5.645	-1.181	1.205	1.946	-0.615	-1.331	-0.315	1.272/ 0.701	0.947/0.801
NKX-2677-P1	5.900	-0.951	1.460	1.971	-0.705	-1.266	-0.405	1.315/ 0.874	0.952/0.866
NKX-2677-P2	6.439	-0.410	1.999	1.969	-0.851	-1.118	-0.551	0.775/ 0.619	0.832/0.759
NKX-2700	5.453	-1.292	1.013	1.864	-0.527	-1.338	-0.227	1.650/ 0.831	0.978/0.853
NKX-2700-P1	5.708	-0.980	1.268	1.808	-0.619	-1.190	-0.319	1.410/ 0.992	0.961/0.898
NKX-2700-P2	6.255	-0.548	1.815	1.923	-0.813	-1.110	-0.513	0.902/ 1.399	0.875/0.960
NKX-2883	5.668	-1.121	1.228	1.910	-0.721	-1.188	-0.421	1.725/ 0.491	0.981/0.677
NKX-2883-P1	5.930	-0.831	1.490	1.881	-0.798	-1.084	-0.498	1.382/0.664	0.959/0.783
NKX-2883-P2	6.387	-0.469	1.947	1.976	-0.942	-1.034	-0.642	1.102/0.909	0.921/0.877
NKX-2883-Q1	5.780	-1.019	1.340	1.919	-0.740	-1.178	-0.440	1.424/ 0.834	0.962/0.854
NKX-2883-Q2	6.067	-0.899	1.627	2.085	-0.840	-1.245	-0.540	0.953/ 1.126	0.889/0.925

[a]Calculated Gibbs free energy change ($\Delta G_{(aq)}$, in V) due to the oxidation of the dyes in aqueous solutions. [b]The driving force(ΔG^0, in V) electron injection related to the electronic transition in B1 band. [c]Redox potential (E_{redox} vs NHE, in V). [d] The vertical excitation energy (ΔE_{ver}, eV) corresponding to the maximum wavelength of spectral absorption. [e]The oxidized potential (vs. NHE, $E_{ox(dye)}$, in eV) of ground state. [f]The oxidized potential of the first excited state ($E_{ox(dye^*)}$) following unrelax path for dyes.[g]The regeneration energy(ΔG_{reg} , in V). [h] The oscillation strength of the two major absorption bands (B1 and B2 bands).[i]The light harvest efficiency (*LHE*) corresponding to B1/B2 bands.

Table 8S Electronic transition data obtained by TD-B3LYP/6-31g(d,p) level for all free dyes and dye-titania complexes in ethanol solution with B3LYP/6-31g(d,p) geometries

Transition energy(eV)	Wavelength/nm	Oscillator strength/ Light harvest efficiency	Wavelength
NKX-2311			
2.468($S_0 \rightarrow S_1$)	502	1.553/0.972	HOMO->LUMO (100%)
3.467($S_0 \rightarrow S_3$)	358	0.138/0.272	H-2->LUMO (31%), HOMO->L+1 (65%)
3.798($S_0 \rightarrow S_4$)	326	0.173/0.329	H-2->LUMO (27%), H-1->LUMO (43%), HOMO->L+1 (23%)
5.963($S_0 \rightarrow S_{27}$)	208	0.504/0.687	H-5->L+1 (14%), H-2->L+2 (52%), H-1->L+2 (15%), HOMO->L+6 (6%)
6.223($S_0 \rightarrow S_{30}$)	199	0.142/0.279	H-14->LUMO (11%), H-2->L+3 (58%), H-5->L+1 (5%), H-2->L+2 (5%)
NKX-2311/TiO_2			
2.146($S_0 \rightarrow S_1$)	578	1.470	HOMO->LUMO (96%)
2.316($S_0 \rightarrow S_4$)	535	0.123	HOMO->L+3 (95%)
NKX-2677			
1.946($S_0 \rightarrow S_1$)	637	1.272/0.947	HOMO->LUMO (100%)
2.725($S_0 \rightarrow S_2$)	455	0.701/0.801	H-1->LUMO (58%), HOMO->L+1 (42%)
3.026($S_0 \rightarrow S_3$)	409	0.117/0.236	H-1->LUMO (42%), HOMO->L+1 (56%)
NKX-2677-TiO_2			
1.757($S_0 \rightarrow S_1$)	705	1.409/0.961	HOMO->LUMO (100%)
2.574($S_0 \rightarrow S_{14}$)	482	0.174/0.330	H-1->LUMO (15%), HOMO->L+13 (79%)
2.582($S_0 \rightarrow S_{15}$)	480	0.547/0.716	H-1->LUMO (63%), HOMO->L+13 (20%), HOMO->L+23 (6%)
NKX-2677-P1			
1.971($S_0 \rightarrow S_1$)	629	1.315/0.952	HOMO->LUMO (100%)
2.806($S_0 \rightarrow S_2$)	442	0.874/0.866	H-1->LUMO (34%), HOMO->L+1 (65%)
4.115($S_0 \rightarrow S_{11}$)	301	0.141/0.277	H-5->LUMO (72%), H-1->L+1 (14%)
4.910($S_0 \rightarrow S_{23}$)	253	0.123/0.247	H-5->L+1 (12%), HOMO->L+5 (60%), H-1->L+3 (5%)
NKX-2677-P2			
1.969($S_0 \rightarrow S_1$)	630	0.775/0.832	HOMO->LUMO (100%)
2.916($S_0 \rightarrow S_2$)	425	0.320/0.521	H-2->LUMO (51%), H-1->LUMO (17%), HOMO->L+1 (24%)
2.932($S_0 \rightarrow S_3$)	423	0.619/0.760	H-2->LUMO (36%), HOMO->L+1 (49%),H-3->LUMO (6%), H-1->LUMO (5%)
2.025($S_0 \rightarrow S_4$)	410	0.116/0.234	H-1->LUMO (75%), HOMO->L+1 (15%)
3.321($S_0 \rightarrow S_6$)	373	0.193/0.359	H-3->LUMO (20%), HOMO->L+2 (76%)
3.420($S_0 \rightarrow S_7$)	362	0.205/0.376	H-3->LUMO (68%), HOMO->L+2 (21%),HOMO->L+1 (9%)
4.052($S_0 \rightarrow S_{13}$)	306	0.176/0.333	H-6->LUMO (17%), H-5->LUMO (68%),H-3->L+1 (5%)
NKX-2700			
1.864($S_0 \rightarrow S_1$)	665	1.650/0.978	HOMO->LUMO (100%)
2.571($S_0 \rightarrow S_2$)	482	0.831/0.852	H-1->LUMO (65%), HOMO->L+1 (34%)
2.862($S_0 \rightarrow S_3$)	433	0.103/0.211	H-1->LUMO (34%), HOMO->L+1 (63%)
NKX-2700/TiO2			
1.696($S_0 \rightarrow S_1$)	731	1.783/0.984	HOMO->LUMO (100%)
2.332($S_0 \rightarrow S_{10}$)	532	0.116/0.234	HOMO->L+8 (12%), HOMO->L+9 (80%)
2.424($S_0 \rightarrow S_{12}$)	512	0.629/0.765	H-1->LUMO (64%), HOMO->L+11 (22%)
2.424($S_0 \rightarrow S_{13}$)	511	0.155/0.300	H-1->LUMO (17%), HOMO->L+11 (74%)

NKX-2700-P1			
1.808(S_0→S_1)	686	1.410/0.961	HOMO->LUMO (100%)
2.619(S_0→S_2)	473	0.992/0.898	H-1->LUMO (56%), HOMO->L+1 (43%)
3.577(S_0→S_8)	347	0.115/0.233	H-3->LUMO (41%), H-1->L+1 (52%)
NKX-2700-P2			
1.923(S_0-S_1)	645	0.902/0.875	HOMO->LUMO (100%)
2.783(S_0-S_2)	445	1.399/0.960	H-1->LUMO (27%), HOMO->L+1 (68%)
NKX-2883			
1.909(S_0→S_1)	649.5	1.725/0.981	HOMO->LUMO (100%)
2.478(S_0→S_2)	500	0.491/0.677	H-1->LUMO (27%), HOMO->L+1 (72%)
2.809(S_0→S_3)	441	0.149/0.290	H-1->LUMO (73%), HOMO->L+1 (27%)
3.679(S_0→S_7)	337	0.100/0.206	H-4->LUMO (14%), H-3->LUMO (37%), HOMO->L+2 (32%), H-1->L+1 (8%)
4.039(S_0→S_{11})	307	0.143/0.280	H-3->L+1 (29%), HOMO->L+3 (56%), H-5->LUMO (8%)
NKX-2883/TiO_2			
1.761	704	1.802/0.984	HOMO->LUMO (99%)
2.368	523	0.344/0.547	H-1->LUMO (12%), HOMO->L+7 (50%), HOMO->L+8 (30%)
2.389	519	0.244/0.430	H-1->LUMO (11%), HOMO->L+7 (47%), HOMO->L+8 (34%)
NKX-2883-P1			
1.881(S_0→S_1)	656	1.382/0.959	HOMO->LUMO (100%)
2.522(S_0→S_2)	491	0.664/0.783	H-1->LUMO (16%), HOMO->L+1 (84%)
2.903(S_0→S_3)	427	0.233/0.415	H-1->LUMO (82%), HOMO->L+1 (16%)
3.861(S_0→S_{11})	321	0.212/0.386	H-5->LUMO (34%), H-3->LUMO (38%), H-1->L+1 (12%), HOMO->L+3 (8%)
4.088(S_0→S_{12})	301	0.179/0.338	HOMO->L+4 (89%)
NKX-2883-P1/TiO_2			
1.772(S_0→S_1)	670	1.404/0.961	HOMO->LUMO (99%)
2.419(S_0→S_8)	512	0.293/0.491	HOMO->L+7 (65%), HOMO->L+8 (24%), H-1->LUMO (5%)
2.448(S_0→S_9)	506	0.264/0.455	HOMO->L+7 (33%), HOMO->L+8 (56%), H-1->LUMO (6%)
2.580(S_0→S_{11})	481	0.149/0.290	H-1->LUMO (12%), HOMO->L+8 (11%), HOMO->L+10(32%), HOMO->L+11(15%), HOMO->L+12 (25%)
2.8065(S_0→S_{16})	442	0.212/0.386	H-1->LUMO (59%), HOMO->L+14 (17%), HOMO->L+12 (9%), HOMO->L+13 (6%)
NKX-2883-P2			
1.976(S_0→S_1)	628	1.102/0.921	HOMO->LUMO (100%)
2.596(S_0→S_2)	478	0.909/0.877	HOMO->L+1 (94%)
3.201(S_0→S_5)	387	0.365/0.568	H-2->LUMO (74%), H-1->LUMO (19%)
3.753(S_0→S_{10})	330	0.146/0.286	H-4->LUMO (50%), H-2->L+1 (35%), H-1->L+1 (10%)
3.936(S_0→S_{13})	315	0.166/0.318	H-4->LUMO (40%), H-2->L+1 (21%), H-1->L+1 (15%), HOMO->L+3 (13%), HOMO->L+4 (6%)
4.209(S_0→S_{16})	295	0.116/0.234	HOMO->L+5 (90%)
NKX-2883-P2/TiO_2			
1.8773(S_0→S_1)	660	1.060/0.913	HOMO->LUMO (99%)
2.4934(S_0→S_6)	497	0.283/0.479	HOMO->L+5 (82%), HOMO->L+6 (8%)
2.5233(S_0→S_7)	491	0.403/0.605	HOMO->L+5 (17%), HOMO->L+6 (60%), HOMO->L+7 (11%),

			HOMO->L+8 (8%)
2.5640(S_0→S_8)	484	0.146/0.286	HOMO->L+6 (27%), HOMO->L+7 (60%), HOMO->L+8 (10%)
2.5975(S_0→S_9)	477	0.153/0.297	HOMO->L+7 (23%), HOMO->L+8 (71%)
3.1016(S_0→S_{22})	340	0.397/0.599	H-2->LUMO (80%), H-1->LUMO (7%)
NKX-2883-Q1			
1.919(S_0→S_1)	646	1.424/0.962	HOMO->LUMO (99%)
2.453(S_0→S_2)	505	0.834/0.853	HOMO->L+1 (90%), H-1->LUMO (9%)
2.823(S_0→S_3)	439	0.217/0.393	H-1->LUMO (89%), HOMO->L+1 (9%)
3.663(S_0→S_{11})	338	0.115/0.232	H-4->LUMO (43%), H-3->LUMO (17%), HOMO->L+3 (18%), H-2->L+1 (5%), H-1->L+1 (7%)
4.060(S_0→S_{15})	305	0.132/0.262	H-1->L+2 (38%), HOMO->L+4 (53%)
4.593(S_0→S_{24})	270	0.251/0.439	H-3->L+2 (77%), H-2->L+2 (12%)
NKX-2883-Q1/TiO_2			
1.833(S_0→S_1)	676.5	1.361/0.956	HOMO->LUMO (98%)
2.371(S_0→S_8)	523	0.628/0.764	HOMO->L+7 (39%), HOMO->L+8 (49%)
2.402(S_0→S_9)	516	0.166/0.318	HOMO->L+7 (60%), HOMO->L+8 (36%)
2.736(S_0→S_{16})	453	0.136/0.269	H-1->LUMO (51%), HOMO->L+14 (42%)
NKX-2883-Q2			
2.085(S_0→S_1)	595	0.953/0.891	HOMO->LUMO (98%)
2.461(S_0→S_2)	504	1.126/0.925	HOMO->L+1 (95%)
2.891(S_0→S_3)	429	0.413/0.614	H-1->LUMO (94%)
3.357(S_0→S_8)	369	0.129/0.257	H-4->LUMO (63%), H-3->LUMO (24%)
3.625(S_0→S_{12})	342	0.230/0.411	H-5->LUMO (57%), H-3->LUMO (23%)H-4->LUMO (5%)), HOMO->L+6 (6%)
4.504(S_0→S_{28})	275	0.192/0.357	H-8->L+1 (15%), H-4->L+2 (35%), H-2->L+2 (13%), HOMO->L+6 (10%), H-3->L+2 (9%), H-1->L+4 (8%)
NKX-2883-Q2/TiO_2			
1.983(S_0→S_1)	625	0.797/0.840	HOMO->LUMO (97%)
2.395(S_0→S_6)	518	0.492/0.678	HOMO->L+5 (69%), HOMO->L+8 (18%), HOMO->L+7 (6%)
2.421(S_0→S_7)	512	0.664/0.783	HOMO->L+5 (30%), HOMO->L+6 (12%), HOMO->L+7 (11%), HOMO->L+8 (39%)
2.761(S_0→S_{14})	449	0.434/0.631	H-1->LUMO (83%), HOMO->L+13 (5%)

Table 9S Electronic transition data obtained by TD-PBE0/6-31g(d,p) level for all free dyes and dye-titania complexes in ethanol solution with B3LYP/6-31g(d,p) geometries

Transition energy(eV)	Wavelength/nm	Oscillator strength/ Light harvest efficiency	Wavelength
NKX-2311			
2.528($S_0 \rightarrow S_1$)	490	1.626/0.976	HOMO->LUMO (100%)
3.623($S_0 \rightarrow S_3$)	342	0.111/0.226	H-2->LUMO (26%), HOMO->L+1 (70%)
3.893($S_0 \rightarrow S_4$)	319	0.177/0.335	H-2->LUMO (29%), H-1->LUMO (46%), HOMO->L+1 (19%)
6.032($S_0 \rightarrow S_{24}$)	205	0.221/0.399	H-4->L+1 (34%), H-2->L+2 (36%), H-1->L+3 (11%), H-2->L+3 (7%), H-1->L+2 (5%)
6.126($S_0 \rightarrow S_{27}$)	202	0.345/0.548	H-4->L+1 (37%), H-2->L+2 (35%), HOMO->L+6 (12%), H-1->L+2 (6%)
6.266($S_0 \rightarrow S_{28}$)	198	0.125/0.250	H-4->L+1 (15%), H-1->L+3 (69%)
6.405($S_0 \rightarrow S_{30}$)	194	0.118/0.238	H-2->L+3 (67%), H-15->LUMO (9%)
NKX-2311/TiO_2			
2.253($S_0 \rightarrow S_1$)	550	1.886/0.987	HOMO->LUMO (99%)
NKX-2677			
2.047($S_0 \rightarrow S_1$)	606	1.407/0.966	HOMO->LUMO (99%)
2.866($S_0 \rightarrow S_2$)	432	0.614/0.757	H-1->LUMO (56%), HOMO->L+1 (42%)
3.110($S_0 \rightarrow S_3$)	399	0.130/0.259	H-1->LUMO (43%), HOMO->L+1 (56%)
NKX-2677-TiO_2			
1.886($S_0 \rightarrow S_1$)	657	1.634/0.977	HOMO->LUMO (98%)
2.705($S_0 \rightarrow S_9$)	458	0.469/0.660	H-1->LUMO (29%), HOMO->L+8 (45%), HOMO->L+7 (7%)
2.768($S_0 \rightarrow S_{11}$)	448	0.270/0.463	H-1->LUMO (49%), HOMO->L+8 (40%)
NKX-2677-P1			
2.087($S_0 \rightarrow S_1$)	594	1.472/0.966	HOMO->LUMO (99%)
2.942($S_0 \rightarrow S_2$)	421	0.742/0.819	H-1->LUMO (25%), HOMO->L+1 (73%)
4.242($S_0 \rightarrow S_{11}$)	292	0.141/0.277	H-5->LUMO (79%), H-1->L+1 (10%)
5.069($S_0 \rightarrow S_{22}$)	245	0.105/0.215	HOMO->L+5 (75%), H-5->L+1 (6%)
5.341($S_0 \rightarrow S_{27}$)	232	0.106/0.217	H-2->L+3 (83%),H-3->L+2 (6%)
NKX-2677-P2			
2.138($S_0 \rightarrow S_1$)	580	0.911/0.877	HOMO->LUMO (99%)
3.052($S_0 \rightarrow S_2$)	406	0.933/0.883	HOMO->L+1 (84%),H-3->LUMO (6%), H-1->LUMO (6%)
3.521($S_0 \rightarrow S_6$)	352	0.421/0.621	H-3->LUMO (61%), HOMO->L+2 (27%), HOMO->L+1 (5%)
4.222($S_0 \rightarrow S_{12}$)	294	0.108/0.220	H-7->LUMO (11%), H-6->LUMO (14%), H-5->LUMO (60%)
NKX-2700			
1.962($S_0 \rightarrow S_1$)	632	1.825/0.985	HOMO->LUMO (99%)
2.714($S_0 \rightarrow S_2$)	457	0.710/0.805	H-1->LUMO (66%), HOMO->L+1 (32%)
2.955($S_0 \rightarrow S_3$)	420	0.122/0.225	H-1->LUMO (33%), HOMO->L+1 (65%)
NKX-2700/TiO2			
1.818($S_0 \rightarrow S_1$)	682	2.062/0.991	HOMO->LUMO (98%)
2.551($S_0 \rightarrow S_7$)	486	0.110/0.224	HOMO->L+5 (11%), HOMO->L+6 (73%), H-1->LUMO (5%)
2.578($S_0 \rightarrow S_8$)	481	0.621/0.761	H-1->LUMO (60%), HOMO->L+6 (15%), HOMO->L+7 (6%), HOMO->L+8 (5%), HOMO->L+16 (7%)

NKX-2700-P1			
1.925($S_0 \rightarrow S_1$)	644	1.575/0.973	HOMO->LUMO (99%)
2.765($S_0 \rightarrow S_2$)	448	0.891/0.870	H-1->LUMO (50%), HOMO->L+1 (47%)
3.000($S_0 \rightarrow S_3$)	413	0.111/0.226	H-1->LUMO (48%), HOMO->L+1 (51%)
NKX-2700-P2			
2.089($S_0 \rightarrow S_1$)	593	1.080/0.917	HOMO->LUMO (98%)
2.918($S_0 \rightarrow S_2$)	425	1.305/0.950	H-1->LUMO (23%), HOMO->L+1 (70%)
3.201($S_0 \rightarrow S_4$)	387	0.185/0.347	H-1->LUMO (65%), HOMO->L+1 (24%)H-3->LUMO (5%)
4.913($S_0 \rightarrow S_{25}$)	252	0.129/0.257	H-5->L+1 (19%), H-2->L+2 (14%), H-2->L+3 (13%), H-1->L+3 (20%), HOMO->L+6 (12%), H-4->L+1 (5%)
NKX-2883			
1.998($S_0 \rightarrow S_1$)	620	1.897/0.987	HOMO->LUMO (98%)
2.623($S_0 \rightarrow S_2$)	472	0.361/0.564	H-1->LUMO (19%), HOMO->L+1 (79%)
2.893($S_0 \rightarrow S_3$)	429	0.175/0.332	H-1->LUMO (80%), HOMO->L+1 (20%)
3.796($S_0 \rightarrow S_7$)	327	0.108/0.220	H-3->LUMO (42%), HOMO->L+2 (36%), H-4->LUMO (9%), H-1->L+1 (6%)
4.224($S_0 \rightarrow S_{11}$)	294	0.154/0.299	H-3->L+1 (14%), HOMO->L+3 (68%), H-5->LUMO (5%), H-1->L+2 (5%)
NKX-2883/TiO_2			
1.8770($S_0 \rightarrow S_1$)	661	2.080/0.992	HOMO->LUMO (97%)
2.4947($S_0 \rightarrow S_3$)	497	0.390/0.593	H-1->LUMO (10%), HOMO->L+2 (33%), HOMO->L+3(24%), HOMO->L+7(14%), HOMO->L+5 (8%), HOMO->L+6 (5%)
NKX-2883-P1			
1.990($S_0 \rightarrow S_1$)	623	1.568/0.973	HOMO->LUMO (98%)
2.654($S_0 \rightarrow S_2$)	467	0.501/0.684	H-1->LUMO (10%), HOMO->L+1 (88%)
3.030($S_0 \rightarrow S_3$)	409	0.284/0.480	H-1->LUMO (88%), HOMO->L+1 (11%)
4.004($S_0 \rightarrow S_{11}$)	310	0.254/0.443	H-5->LUMO (43%), H-3->LUMO (38%)H-1->L+1 (9%), HOMO->L+3 (6%)
4.263($S_0 \rightarrow S_{13}$)	291	0.151/0.294	HOMO->L+4 (86%)
NKX-2883-P1/TiO_2			
1.907($S_0 \rightarrow S_1$)	650	1.657/0.978	HOMO->LUMO (97%)
2.543($S_0 \rightarrow S_3$)	488	0.477/0.667	HOMO->L+2 (32%), HOMO->L+3 (20%), HOMO->L+5 (14%), HOMO->L+7 (14%), H-1->LUMO (6%), HOMO->L+6 (8%)
2.639($S_0 \rightarrow S_5$)	470	0.108/0.220	HOMO->L+3 (51%), HOMO->L+5 (15%), HOMO->L+4 (8%), HOMO->L+6 (6%), HOMO->L+7 (9%)
2.907($S_0 \rightarrow S_{10}$)	426.5	0.230/0.411	H-1->LUMO (53%), HOMO->L+7 (12%) HOMO->L+10 (15%), HOMO->L+8 (7%), HOMO->L+11(7%)
2.973($S_0 \rightarrow S_{12}$)	417	0.130/0.259	H-1->LUMO (26%), HOMO->L+10 (65%), HOMO->L+11 (5%)
NKX-2883-P2			
2.122($S_0 \rightarrow S_1$)	584	1.371/0.957	HOMO->LUMO (98%)
2.711($S_0 \rightarrow S_2$)	457	0.653/0.778	HOMO->L+1 (94%)
3.360($S_0 \rightarrow S_5$)	369	0.468/0.660	H-2->LUMO (71%), H-1->LUMO (20%)
4.017($S_0 \rightarrow S_{11}$)	309	0.160/0.308	H-4->LUMO (34%), H-2->L+1 (11%), HOMO->L+4 (34%),H-1->L+1 (9%), HOMO->L+3 (5%)
4.386($S_0 \rightarrow S_{17}$)	283	0.106/0.308	HOMO->L+5 (84%), HOMO->L+6 (8%)
NKX-2883-P2/TiO_2			

2.049($S_0 \rightarrow S_1$)	605	1.367/0.957	HOMO->LUMO (97%)
2.638($S_0 \rightarrow S_2$)	470	0.682/0.792	HOMO->L+1 (18%), HOMO->L+2 (18%), HOMO->L+4 (16%), HOMO->L+5(32%), HOMO->L+3(6%)
2.649($S_0 \rightarrow S_3$)	468	0.131/0.260	HOMO->L+1 (81%), HOMO->L+2 (6%), HOMO->L+5 (6%)
3.279($S_0 \rightarrow S_{16}$)	378	0.426/0.625	H-2->LUMO (69%), HOMO->L+13 (15%)
NKX-2883-Q1			
2.042($S_0 \rightarrow S_1$)	607	1.695/0.980	HOMO->LUMO (96%)
2.581($S_0 \rightarrow S_2$)	480	0.577/0.735	HOMO->L+1 (92%)
2.961($S_0 \rightarrow S_3$)	418	0.293/0.491	H-1->LUMO (92%), HOMO->L+1(5%)
3.785($S_0 \rightarrow S_{10}$)	328	0.173/0.329	H-4->LUMO (57%), H-3->LUMO (16%), H-2->L+1(5%)), HOMO->L+3(6%)
4.219($S_0 \rightarrow S_{14}$)	294	0.156/0.302	HOMO->L+4 (71%), H-7->LUMO (9%), H-4->L+1 (6%), H-1->L+2 (5%)
4.760($S_0 \rightarrow S_{24}$)	260	0.309/0.509	H-3->L+2 (79%), H-2->L+2 (5%)
NKX-2883-Q1/TiO_2			
1.987($S_0 \rightarrow S_1$)	624	1.756/0.982	HOMO->LUMO (95%)
2.500($S_0 \rightarrow S_3$)	496	0.552/0.719	HOMO->L+2 (21%), HOMO->L+3 (19%), HOMO->L+5 (16%), HOMO->L+6 (20%), HOMO->L+1 (7%), HOMO->L+7 (8%)
2.876($S_0 \rightarrow S_{10}$)	431	0.348/0.551	H-1->LUMO (72%)，HOMO->L+9 (6%), HOMO->L+10 (7%)
NKX-2883-Q2			
2.244($S_0 \rightarrow S_1$)	552	1.430/0.963	HOMO->LUMO (90%), HOMO->L+1 (8%)
2.581($S_0 \rightarrow S_2$)	480	0.668/0.785	HOMO->L+1 (89%), HOMO->LUMO (9%)
3.043($S_0 \rightarrow S_3$)	407	0.541/0.712	H-1->LUMO (93%)
3.548($S_0 \rightarrow S_8$)	349.5	0.145/0.284	H-4->LUMO (48%), H-3->LUMO (27%), HOMO->L+2 (9%)
3.758($S_0 \rightarrow S_{10}$)	330	0.128/0.255	H-5->LUMO (27%), H-2->LUMO (33%), H-2->L+1 (21%), HOMO->L+3 (5%)
4.069($S_0 \rightarrow S_{15}$)	305	0.137/0.271	H-4->L+1 (29%), H-3->L+1 (40%), HOMO->L+4 (18%)
4.263($S_0 \rightarrow S_{18}$)	291	0.103/0.211	H-5->L+1 (18%), H-1->L+2 (13%), HOMO->L+5 (50%), HOMO->L+4 (5%)
4.700($S_0 \rightarrow S_{28}$)	264	0.273/0.467	H-4->L+2 (40%), H-3->L+2 (19%), H-2->L+2 (16%)
NKX-2883-Q2/TiO_2			
2.180($S_0 \rightarrow S_1$)	569	1.346/0.955	HOMO->LUMO (91%)
2.524($S_0 \rightarrow S_2$)	491	0.953/0.889	HOMO->L+3(12%), HOMO->L+4(11%), HOMO->L+5(50%), HOMO->LUMO (8%), HOMO->L+2(6%), HOMO->L+6(5%)
2.937($S_0 \rightarrow S_{10}$)	422	0.716/0.808	H-1->LUMO (91%)
3.491($S_0 \rightarrow S_{26}$)	355	0.117/0.236	H-4->LUMO (36%), H-3->LUMO (17%), HOMO->L+19 (30%)

Table 10S Electron density difference plots of electronic transition $S_0 \rightarrow S_1$ for each coumarin dyes performed in ethanol solution using the B3LYP functional with 6-31G(d,p) basis set. L is the electron transfer distance (Å); Δe is the fraction of electron exchange ($|e^-|$), Ω is overlaps between the regions of density depletion and increment. (Isovalue: 4×10^{-4} e au^{-3})

Molecule	picture	*f*	*L*	Δ*e*	*Ω*
NKX-2311	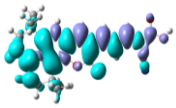	1.553	4.514	1.034	0.425
NKX-2677	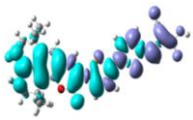	1.272	9.367	1.129	0.170
NKX-2677-P1	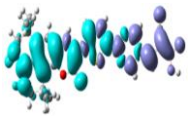	1.315	10.389	1.223	0.117
NKX-2677-P2	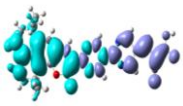	0.775	11.800	1.364	0.026
NKX-2700	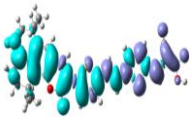	1.650	10.301	1.101	0.200
NKX-2700-P1	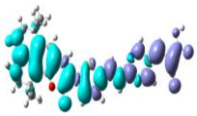	1.410	11.515	1.211	0.104
NKX-2700-P2	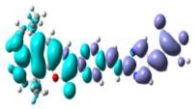	0.902	13.075	1.357	0.028
NKX-2833	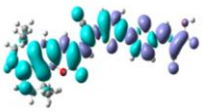	1.725	9.024	1.070	0.372
NKX-2883-P1	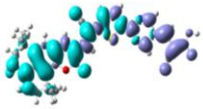	1.382	10.270	1.195	0.200
NKX-2883-P2	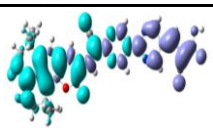	1.102	12.187	1.323	0.077
NKX-2883-Q1	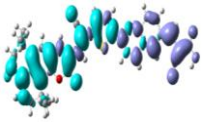	1.424	12.587	1.208	0.118
NKX-2883-Q2	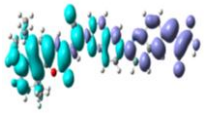	0.953	16.245	1.345	0.018

Table 11S Electron density difference plots of electronic transition $S_0 \rightarrow S_1$ for each coumarin dyes performed in ethanol solution using the PBE0 functional with 6-31G(d,p) basis set. L is the electron transfer distance (Å); Δe is the fraction of electron exchange ($|e^-|$), Ω is overlaps between the regions of density depletion and increment. (Isovalue: 4×10^{-4} e au^{-3})

Molecule	**picture**	***f***	***L*** (Ang)	**Δ*e***	***Ω***
NKX-2311	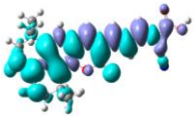	1.626	4.549	1.036	0.422
NKX-2677	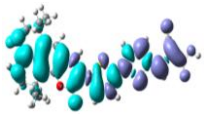	1.407	9.503	1.136	0.151
NKX-2677-P1	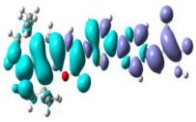	1.472	10.42	1.220	0.108
NKX-2677-P2	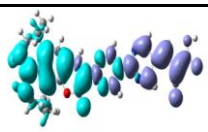	0.911	11.715	1.352	0.027
NKX-2700	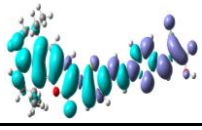	1.825	10.514	1.101	0.177
NKX-2700-P1	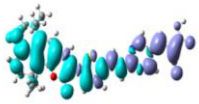	1.575	11.579	1.211	0.094
NKX-2700-P2	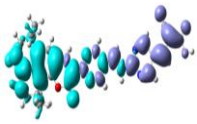	1.080	13.000	1.331	0.027
NKX-2833	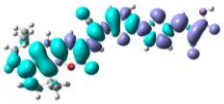	1.897	9.078	1.059	0.364
NKX-2883-P1	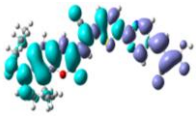	1.568	10.228	1.174	0.195
NKX-2883-P2	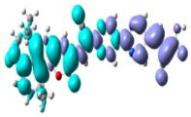	1.371	12.026	1.291	0.085
NKX-2883-Q1	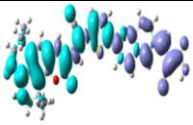	1.698	12.510	1.174	0.120
NKX-2883-Q2	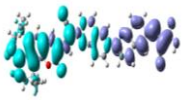	1.430	15.691	1.304	0.040

Table 12S Electron density difference plots of electron transitions with oscillation strength larger than 0.1 for all dyes using M062X functional

NKX-2311			
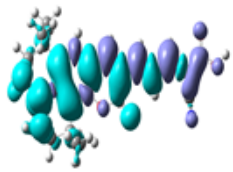	*L* = 5.164 Ang Δ*e* = 1.024 Ω= 0.376 *f*=1.774	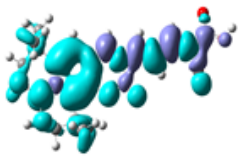	*L*=4.857 Ang Δ*e*=0.812 Ω= 0.427 *f*=0.180
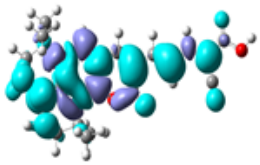	*L*= 0.470 Ang Δ*e*= 0.765 Ω= 0.880 *f*=0.110	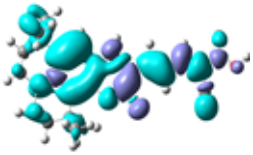	*L*=3.144 Ang Δ*e*=0.754 Ω= 0.727 *f*=0.147
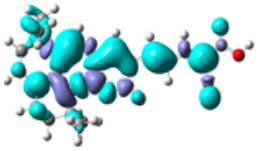	*L* = 1.062 Ang Δ*e*=0.514 Ω= 0.877 *f*=0.314	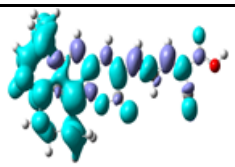	*L*=4.041Ang Δ*e*=0.445 Ω= 0.599 *f*=0.101
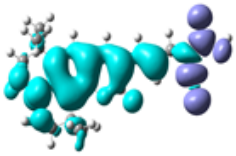	*L*= 8.667 Ang Δ*e*= 1.110 Ω= 0.026 *f*=0.116	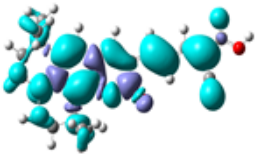	*L*=1.096 Ang Δ*e*=0.674 Ω= 0.887 *f*=0.139

NKX-2677		NKX-2677-P1		NKX-2677-P2	
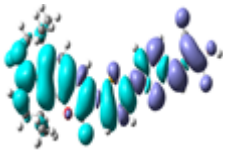	*L*=9.748Ang Δ*e*=1.118 Ω=0.137 *f*=1.851	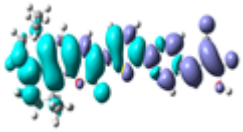	*L*=10.449 Ang Δ*e*=1.149 Ω=0.110 *f*=2.067	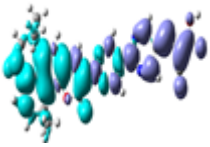	*L*=11.244 Ang Δ*e*=1.197 Ω=0.059 *f*=1.789
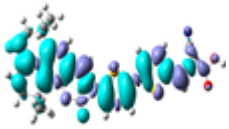	*L*=5.257 Ang Δ*e*=0.825 Ω=0.751 *f*=0.177	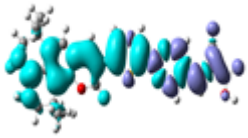	*L*=8.898 Ang Δ*e*=0.941 Ω=0.320 *f*=0.277	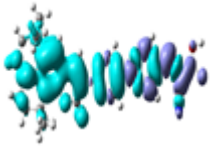	*L*=8.624Ang Δ*e*=0.900 Ω=0.268 *f*=0.678
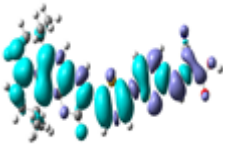	*L*=7.423 Ang Δ*e*=0.806 Ω=0.504 *f*=0.180	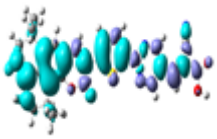	*L*=7.492 Ang Δ*e*=0.700 Ω=0.517 *f*=0.104	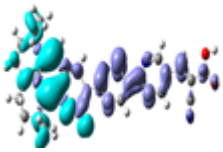	*L*=7.404 Ang Δ*e*=0.734 Ω=0.191 *f*=0.446
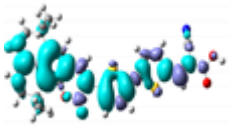	*L*=6.699 Ang Δ*e*=0.6270 Ω=0.5899 *f*=0.1317	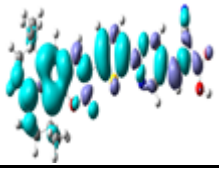	*L*=7.192 Ang Δ*e*=0.5873 Ω=0.5707 *f*=0.1339		

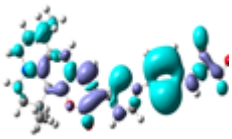	*L*=3.737 Ang Δ*e*=0.592 Ω=0.808 *f*=0.112	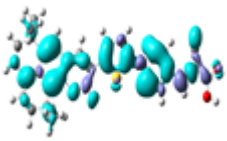	*L*=4.753 Ang Δ*e*=0.483 Ω=0.786 *f*=0.175
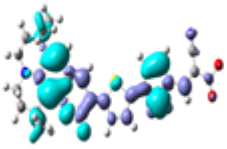	*L*=4.001 Ang Δ*e*=0.515 Ω=0.817 *f*=0.213	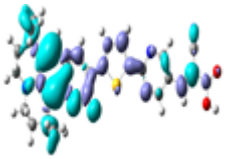	*L*=5.057 Ang Δ*e*=0.565 Ω=0.654 *f*=0.557
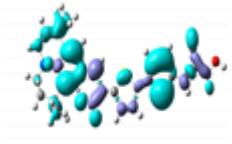	*L*=1.158 Ang Δ*e*=0.553 Ω=0.930 *f*=0.320		

NKX-2700		NKX-2700-P1		NKX-2700-P2	
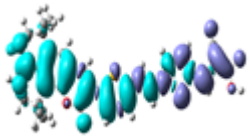	*L*=10.995 Ang Δ*e*=1.060 Ω= 0.143 *f*=2.347	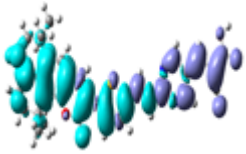	*L*=11.841 Ang Δ*e*=1.166 Ω= 0.076 *f*=2.194	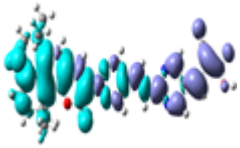	*L*=12.812 Ang Δ*e*=1.155 Ω= 0.052 *f*=2.178
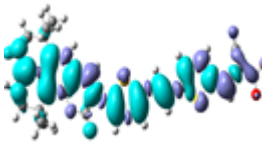	*L*=6.517 Ang Δ*e*=0.803 Ω= 0.718 *f*=0.170	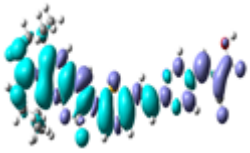	*L*=8.254 Ang Δ*e*=0.873 Ω= 0.516 *f*=0.162	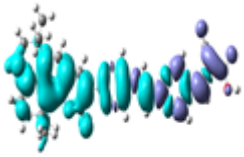	*L*=11.418Ang Δ*e*=0.899 Ω= 0.145 *f*=0. 578
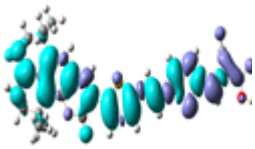	*L*=8.829 Ang Δ*e*=0.813 Ω= 0.481 *f*=0.202	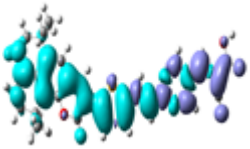	*L*=10.661 Ang Δ*e*=0.931 Ω= 0.166 *f*=0.334	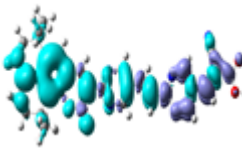	*L*=10.746 Ang Δ*e*=0.663 Ω= 0.257 *f*=0.155
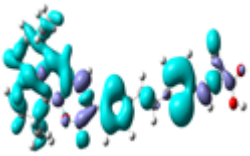	*L*=2.078 Ang Δ*e*=0.515 Ω=902 *f*=0.117	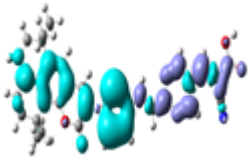	*L*=8.705 Ang Δ*e*=0.712 Ω= 0.181 *f*=0.132		
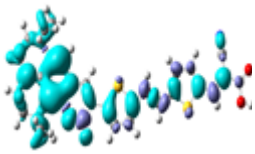	*L*= 6.798 Ang Δ*e*=0.548 Ω= 0.611 *f*=0.174	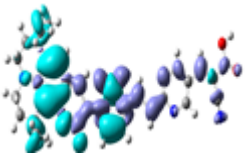	*L*=7.121 Ang Δ*e*=0.802 Ω= 0.391 *f*=0.373		
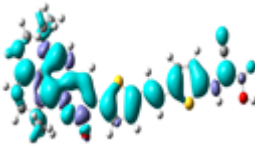	*L*=0.750Ang Δ*e*=0.555 Ω= 0.938 *f*=0.325				

NKX-2883		NKX-2883-P1		NKX-2883-P2	
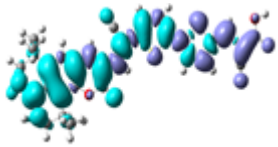	*L*= 9.403 Ang Δ*e*=0.100 Ω= 0.350 *f*=2.255	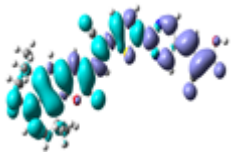	*L*=10.405Ang Δ*e*=1.120 Ω= 0.192 *f*=2.001	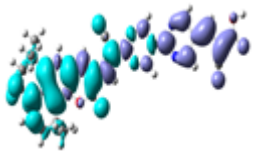	*L*=11.182 Ang Δ*e*=1.144 Ω=0.168 *f*=2.024
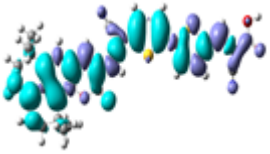	*L*= 6.432 Ang Δ*e*= 0.838 Ω= 0.723 *f*=0.144	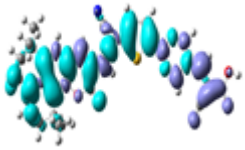	*L*=7.947 Ang Δ*e*=0.876 Ω= 0.545 *f*=0.203	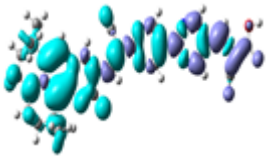	*L*=10.673 Ang Δ*e*=0.830 Ω= 0.242 *f*=0.242
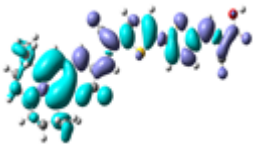	*L*= 7.291 Ang Δ*e*= 0.828 Ω= 0.551 *f*=0.105	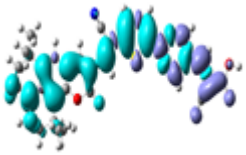	*L*=8.937 Ang Δ*e*=0.841 Ω= 0.306 *f*=0.206	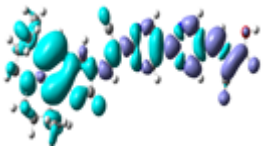	*L*=11.191Ang Δ*e*=0.811 Ω= 0.172 *f*=0.376
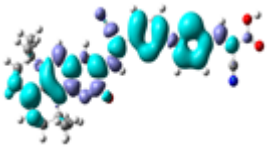	*L*= 0.250 Ang Δ*e*= 0.625 Ω= 0.978 *f*=0.194	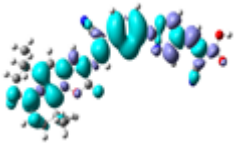	*L*=6.353 Ang Δ*e*=0.649 Ω= 0.680 *f*=0.295	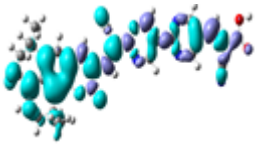	*L*=8.224 Ang Δ*e*=0.704 Ω= 0.513 *f*=0.0.240
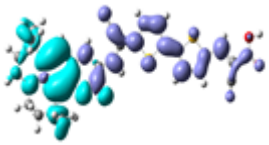	*L*= 8.743 Ang Δ*e*=0.952 Ω= 0.130 *f*=0.337				

NKX-2883-Q1		NKX-2883-Q2	
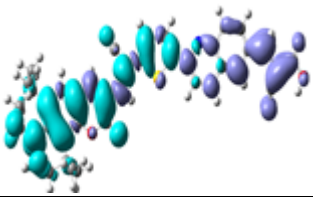	*L*=11.782 Ang Δ*e*=1.050 Ω= 0.216 *f*=2.270	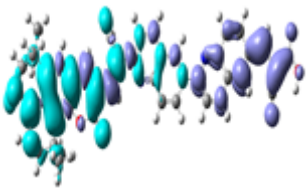	*L*=12.934 Ang Δ*e*=1.073 Ω= 0.241 *f*=2.117
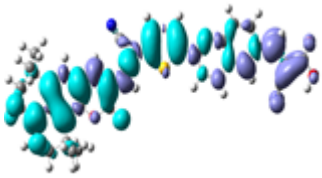	*L*=9.596 Ang Δ*e*=0.872 Ω= 0.495 *f*=0.199	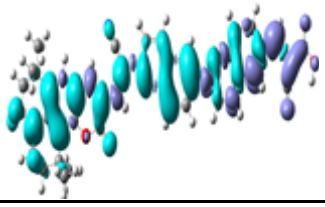	*L*=11.184 Ang Δ*e*=0.816 Ω= 0.472 *f*=0.607
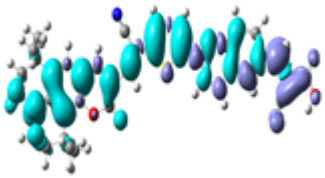	*L*=10.275 Ang Δ*e*=0.794 Ω= 0.349 *f*=0.227	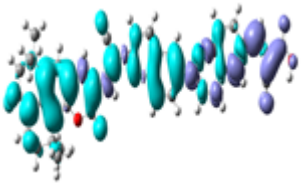	*L*=13.666 Ang Δ*e*=0.843 Ω= 0.236 *f*=0.226
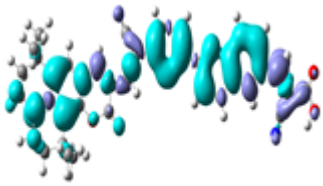	*L*=5.455ng Δ*e*= 0.649 Ω= 0.825 *f*=0.171	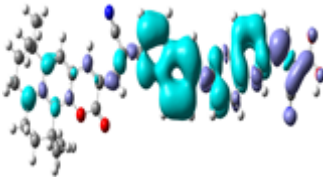	*L*=5.586 Ang Δ*e*=0.601 Ω= 0.750 *f*=0.102

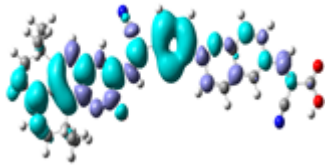	*L*=3.398 Ang Δ*e*=0.620 Ω= 0.898 *f*=0.220	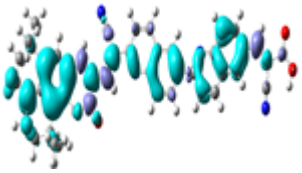	*L*= 5.262 Ang Δ*e*= 0.484 Ω= 0.852 *f*=0.149
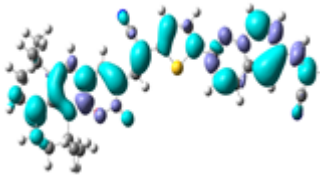	*L*=1.789 Ang Δ*e*=0.410 Ω= 0.982 *f*=0.295	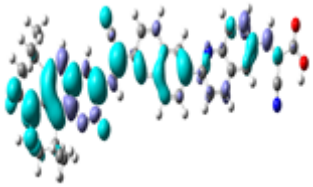	*L*=4.529 Ang Δ*e*=0.480 Ω= 0.852 *f*=0.201
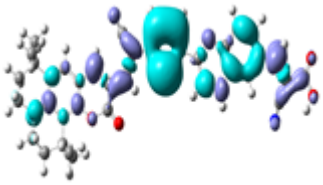	*L*=1.282 Ang Δ*e*=0.650 Ω= 0.801 *f*=0.133	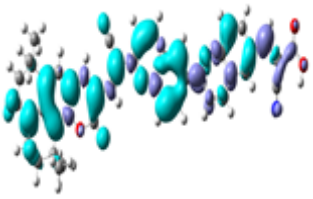	*L*=8.734 Ang Δ*e*= 0.619 Ω= 0.634 *f*=0.175
		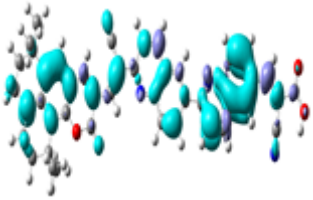	*L*=4.787 Ang Δ*e*=0.405 Ω= 0.869 *f*=0.448
		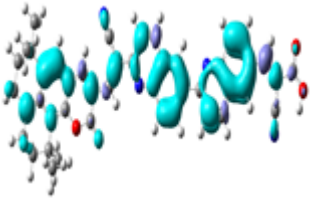	*L*=4.687Ang Δ*e*=0.334 Ω= 0.904 *f*=0.253
		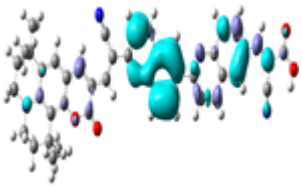	*L*=0.243 Ang Δ*e*=0.287 Ω= 0.942 *f*=0.256

Table 13S Electron density difference plots of electron transitions with oscillation strength larger than 0.1 for all dyes using B3LYP functional

NKX-2311			
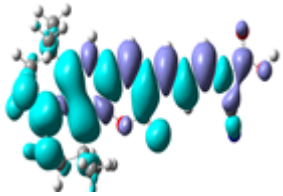	*L* = 4.514 Ang Δ*e* = 1.034 Ω= 0.425 *f*=1.553	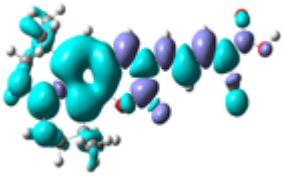	*L*=4.321 Ang Δ*e*=0.846 Ω= 0.583 *f*=0.138
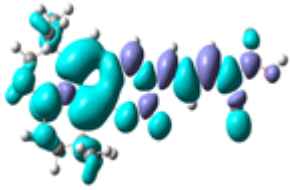	*L*= 4.473 Ang Δ*e*= 0.764 Ω= 0.504 *f*=0.173	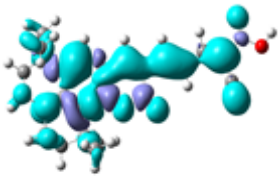	*L*=1.265Ang Δ*e*=0.600 Ω= 0.897 *f*=0.504
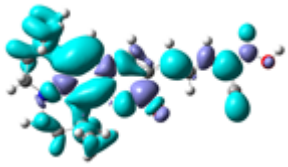	*L* =2.013 Ang Δ*e*= 0.634 Ω= 0.824 *f*=0.142		

NKX-2677		NKX-2677-P1		NKX-2677-P2	
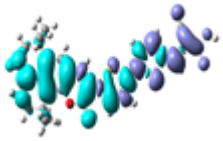	*L*=9.367 Ang Δ*e*=1.129 Ω=0.170 *f*=1.272	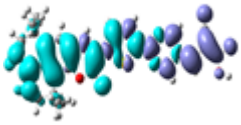	*L*=10.389 Ang Δ*e*=1.223 Ω=0.117 *f*=1.315	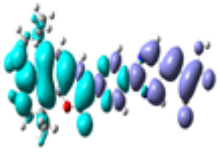	*L*=11.800 Ang Δ*e*=1.364 Ω=0.026 *f*=0.775
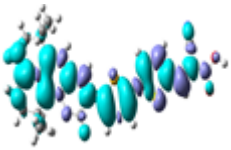	*L*=5.889 Ang Δ*e*=0.819 Ω=0.704 *f*=0.701	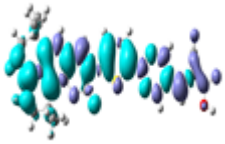	*L*=6.542 Ang Δ*e*=0.883 Ω=0.644 *f*=0.874	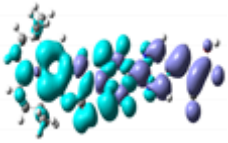	*L*=8.186 Ang Δ*e*=1.144 Ω=0.242 *f*=0.320
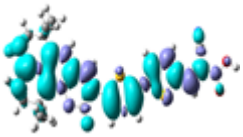	*L*=5.022 Ang Δ*e*=0.811 Ω=0.780 *f*=0.117	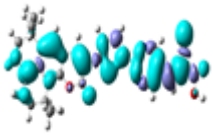	*L*=3.543 Ang Δ*e*=0.606 Ω=0.857 *f*=0.141	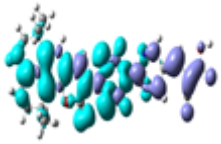	*L*=8.110 Ang Δ*e*=1.038 Ω=0.358 *f*=0.619
		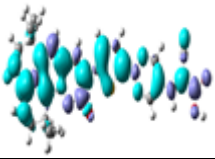	*L*=4.254 Ang Δ*e*=0.631 Ω=0.818 *f*=0.123	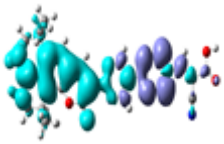	*L*=10.190 Ang Δ*e*=1.168 Ω=0.029 *f*=0.193
				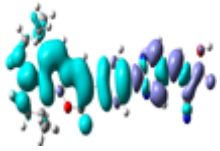	*L*=9.373 Ang Δ*e*=0.903 Ω= 0.197 *f*=0.205

				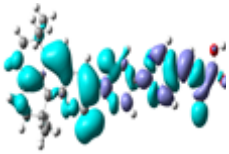	*L*=7.024 Ang Δ*e*=0.771 Ω=0.432 *f*=0.176

NKX-2700		NKX-2700-P1		NKX-2700-P2	
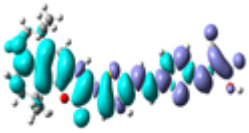	*L*=10.301 Ang Δ*e*=1.101 Ω= 0.200 *f*=1.650	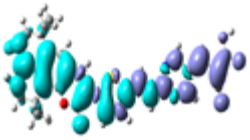	*L*=11.515 Ang Δ*e*=1.211 Ω= 0.104 *f*=1.410	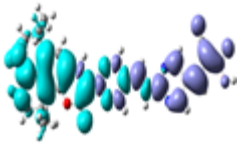	*L*=13.075 Ang Δ*e*=1.357 Ω= 0.028 *f*=0.902
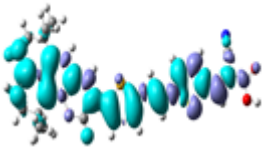	*L*=7.801 Ang Δ*e*=0.818 Ω= 0.605 *f*=0.831	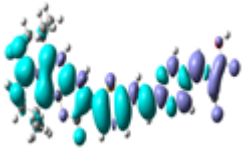	*L*=9.905 Ang Δ*e*=0.905 Ω= 0.328 *f*=0.992	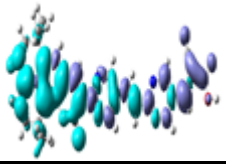	*L*=10.093 Ang Δ*e*=0.925 Ω= 0.340 *f*=1.399
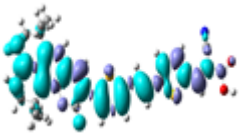	*L*=5.660 Ang Δ*e*=0.809 Ω= 0.774 *f*=0.103	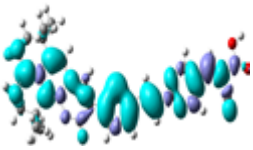	*L*=4.886 Ang Δ*e*=0.681 Ω= 0.842 *f*=0.115		

NKX-2883		NKX-2883-P1		NKX-2883-P2	
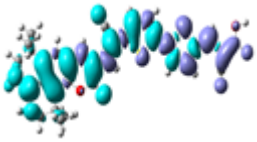	*L*= 9.024 Ang Δ*e*=1.070 Ω= 0.372 *f*=1.725	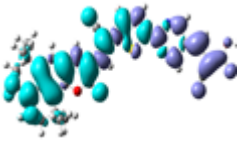	*L*=10.270Ang Δ*e*=1.195 Ω= 0.198 *f*=1.382	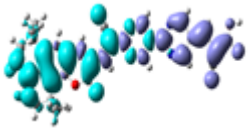	*L*=12.187Ang Δ*e*=1.323 Ω=0.077 *f*=1.102
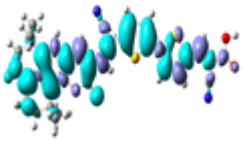	*L*= 5.232 Ang Δ*e*= 0.855 Ω= 0.804 *f*=0.491	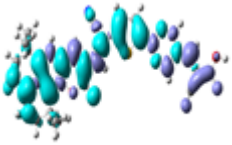	*L*=6.937 Ang Δ*e*=0.950 Ω= 0.643 *f*=0.664	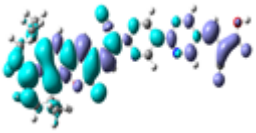	*L*=7.221 Ang Δ*e*=0.983 Ω= 0.548 *f*=0.909
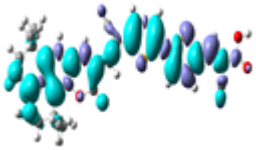	*L*= 6.188 Ang Δ*e*= 0.808 Ω= 0.735 *f*=0.149	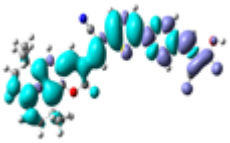	*L*=8.902 Ang Δ*e*=0.902 Ω= 0.342 *f*=0.233	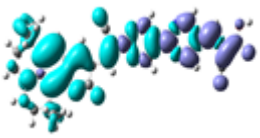	*L*=12.127 Ang Δ*e*=1.020 Ω= 0.061 *f*=0.365
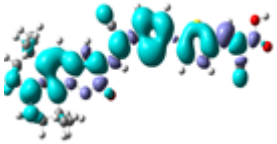	*L*= 5.555 Ang Δ*e*= 0.696 Ω= 0.743 *f*=0.100	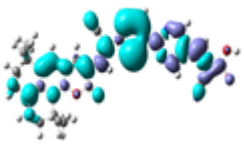	*L*=5.413 Ang Δ*e*=0.766 Ω= 0.628 *f*=0.212	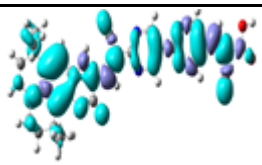	*L*=4.723 Ang Δ*e*=0.698 Ω= 0.823 *f*=0.146
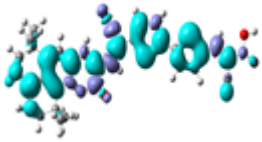	*L*= 2.030 Ang Δ*e*=0.701 Ω= 0.930 *f*=0.143	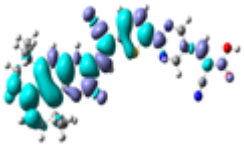	*L*=4.933 Ang Δ*e*=0.862 Ω= 0.714 *f*=0.179	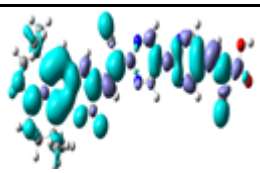	*L*=6.885 Ang Δ*e*=0.702 Ω= 0.674 *f*=0.166

		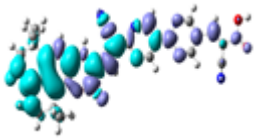	*L*=6.705Ang Δ*e*=0.943 Ω= 0.520 *f*=0.116

NKX-2883-Q1		NKX-2883-Q2	
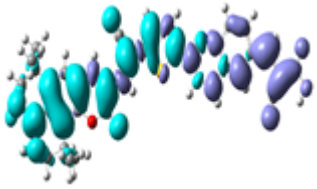	*L*=12.587 Ang Δ*e*=1.208 Ω= 0.118 *f*=1.424	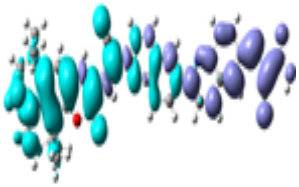	*L*=16.245Ang Δ*e*=1.345 Ω= 0.018 *f*=0.953
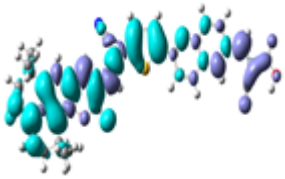	*L*=7.028 Ang Δ*e*=0.964 Ω= 0.689 *f*=0.834	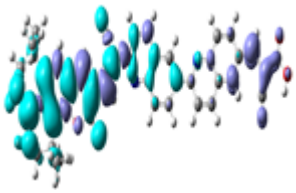	*L*=6.920 Ang Δ*e*=0.972 Ω= 0.600 *f*=1.126
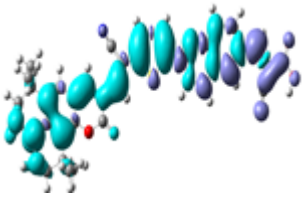	*L*=10.173 Ang Δ*e*=0.952 Ω= 0.320 *f*=0.217	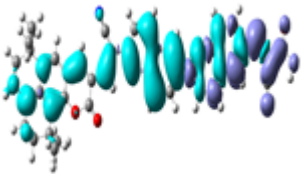	*L*=9.780 Ang Δ*e*=0.964 Ω= 0.317 *f*=0.413
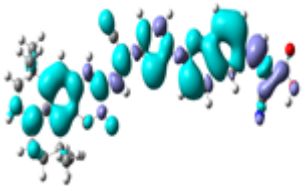	*L*=6.569 Ang Δ*e*= 0.676 Ω= 0.728 *f*=0.115	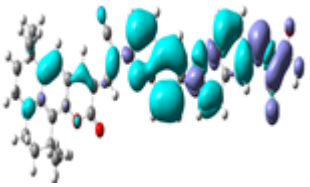	*L*=7.652 Ang Δ*e*=0.795 Ω= 0.504 *f*=0.129
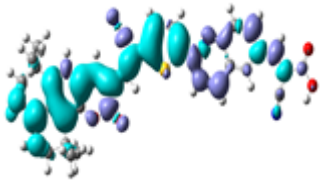	*L*=7.258 Ang Δ*e*=0.818 Ω= 0.642 *f*=0.132	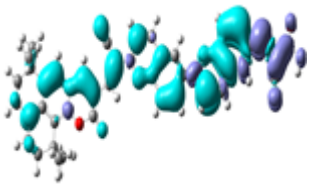	*L*=8.357 Ang Δ*e*=0.834 Ω= 0.564 *f*=0.320
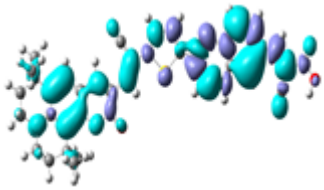	*L*=3.030 Ang Δ*e*=0.806 Ω= 0.807 *f*=0.251	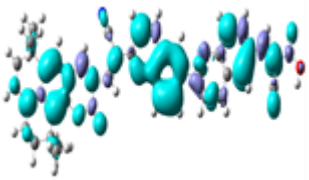	*L*=3.196 Ang Δ*e*=0.616 Ω= 0.903 *f*=0.192

Table 14S The electron density difference plots of electron transitions of all systems using PBE0 functional.

NKX-2311			
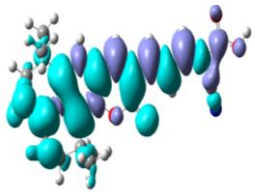	*L* = 4.549 Ang Δ*e* = 1.363 Ω= 0.422 *f*=1.626	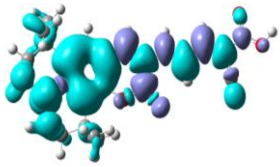	*L*=4.254 Ang Δ*e*=0.854 Ω= 0.593 *f*=0.111
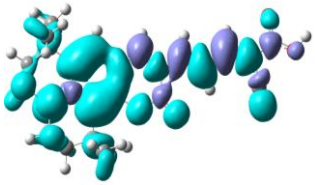	*L*= 4.464 Ang Δ*e*= 0.777 Ω= 0.492 *f*=0.177	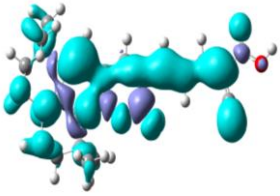	*L*=0.654 Ang Δ*e*=0.631 Ω= 0.892 *f*=0.221
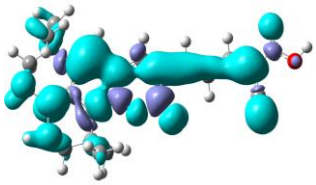	*L* = 0.539 Ang Δ*e*=0.600 Ω= 0.927 *f*=0.345	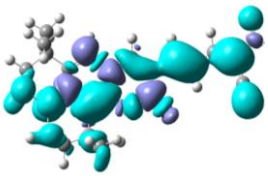	*L*=1.433 Ang Δ*e*=0.747 Ω= 0.850 *f*=0.125
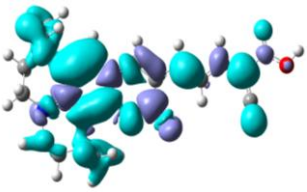	*L*= 1.674 Ang Δ*e*= 0.680 Ω= 0.846 *f*=0.118		

NKX-2677		NKX-2677-P1		NKX-2677-P2	
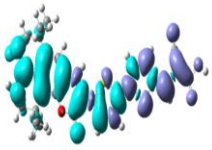	*L*=9.503 Ang Δ*e*=1.136 Ω=0.151 *f*=1.407	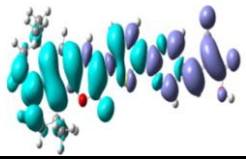	*L*=10.423 Ang Δ*e*=1.220 Ω=0.108 *f*=1.472	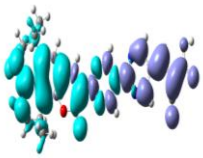	*L*=11.715Ang Δ*e*=1.352 Ω=0.027 *f*=0.911
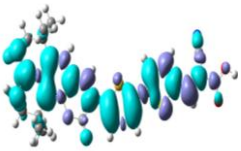	*L*=5.947 Ang Δ*e*=0.809 Ω=0.694 *f*=0.614	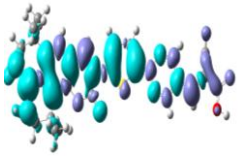	*L*=5.941 Ang Δ*e*=0.889 Ω=0.684 *f*=0.742	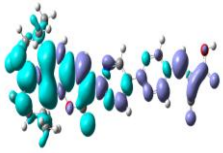	*L*=7.888 Ang Δ*e*=0.947 Ω=0.380 *f*=0.933
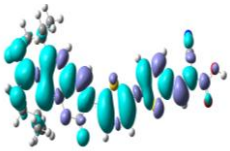	*L*=5.228 Ang Δ*e*=0.825 Ω=0.760 *f*=0.130	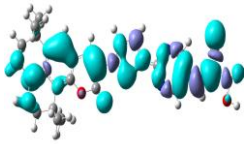	*L*=3.466 Ang Δ*e*=0.642 Ω=0.847 *f*=0.141	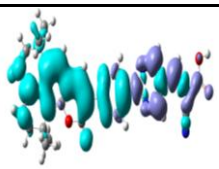	*L*=9.363 Ang Δ*e*=0.877 Ω=0.176 *f*=0.421
		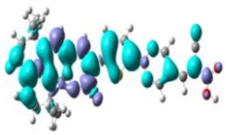	*L*=1.165 Ang Δ*e*=0.697 Ω=0.931 *f*=0.105	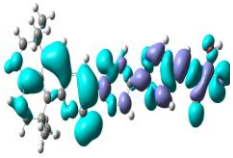	*L*=4.912 Ang Δ*e*=0.774 Ω=0.624 *f*=0.108

	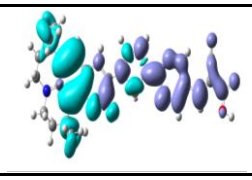	*L*=8.749 Ang Δ*e*=1.087 Ω=0.099 *f*=0.106

NKX-2700		NKX-2700-P1		NKX-2700-P2	
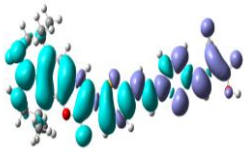	*L*=10.514Ang Δ*e*=1.101 Ω= 0.177 *f*=1.825	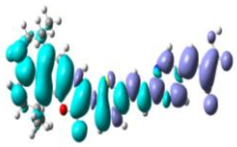	*L*=11.579 Ang Δ*e*=1.211 Ω= 0.094 *f*=1.575	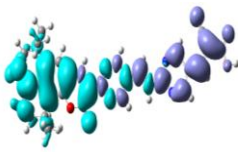	*L*=13.000 Ang Δ*e*=1.331 Ω= 0.027 *f*=1.080
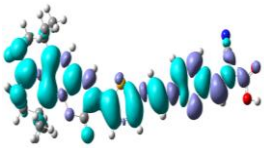	*L*=7.949 Ang Δ*e*=0.818 Ω= 0.583 *f*=0.711	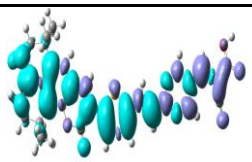	*L*=9.631 Ang Δ*e*=0.892 Ω= 0.366 *f*=0.891	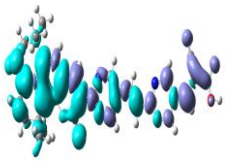	*L*=9.817 Ang Δ*e*=0.910 Ω= 0.360 *f*=1.305
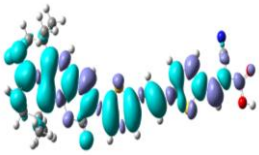	*L*=5.822Ang Δ*e*=0.828 Ω= 0.759 *f*=0.122	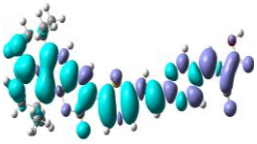	*L*=9.490Ang Δ*e*=0.910 Ω= 0.387 *f*=0.111	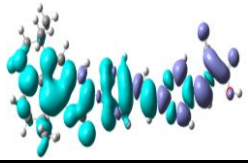	*L*=11.127 Ang Δ*e*=0.906 Ω= 0.170 *f*=0.185
				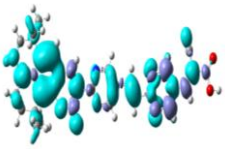	*L*=8.084Ang Δ*e*=0.659 Ω= 0.526 *f*=0.129

NKX-2883		NKX-2883-P1		NKX-2883-P2	
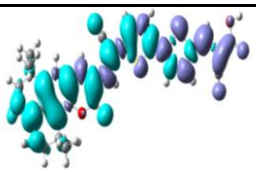	*L*= 9.078 Ang Δ*e*=1.059 Ω= 0.364 *f*=1.897	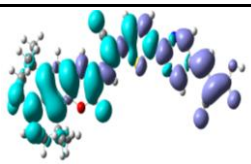	*L*=10.228Ang Δ*e*=1.174 Ω= 0.195 *f*=1.568	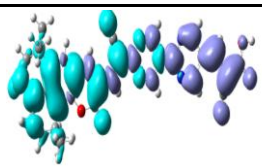	*L*=12.026 Ang Δ*e*=1.291 Ω=0.085 *f*=1.371
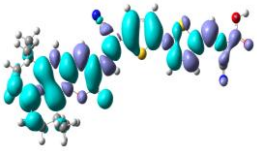	*L*= 5.526 Ang Δ*e*= 0.876 Ω= 0.778 *f*=0.361	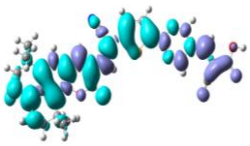	*L*=6.860Ang Δ*e*=0.958 Ω= 0.637 *f*=0.501	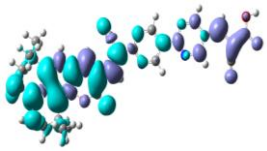	*L*=7.518 Ang Δ*e*=0.992 Ω= 0.528 *f*=0.653
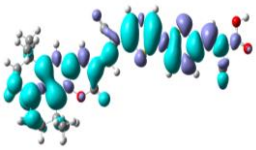	*L*= 5.994 Ang Δ*e*= 0.816 Ω= 0.739 *f*=0.175	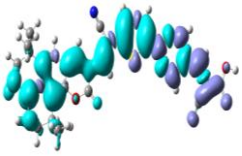	*L*=8.567Ang Δ*e*=0.922 Ω= 0.368 *f*=0.284	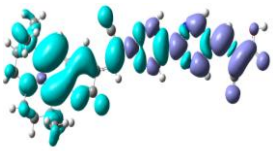	*L*=12.256 Ang Δ*e*=0.991 Ω= 0.063 *f*=0.468
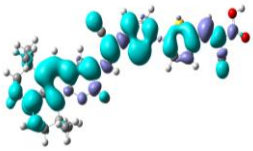	*L*= 6.286 Ang Δ*e*= 0.659 Ω= 0.697 *f*=0.108	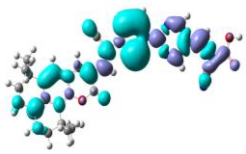	*L*=4.763 Ang Δ*e*=0.834 Ω= 0.656 *f*=0.254	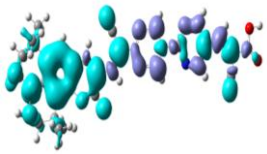	*L*=7.782 Ang Δ*e*=0.818 Ω= 0.462 *f*=0.160

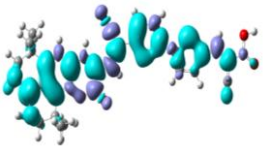	*L*= 2.561 Ang Δ*e*=0.733 Ω= 0.902 *f*=0.154	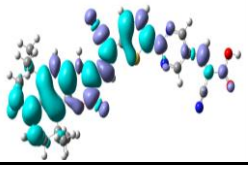	*L*=4.971 Ang Δ*e*=0.831 Ω= 0.709 *f*=0.151	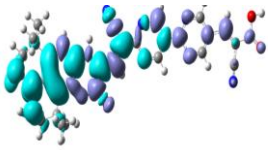	*L*=6.204 Ang Δ*e*=0.939 Ω= 0.577 *f*=0.106

NKX-2883-Q1		**NKX-2883-Q2**	
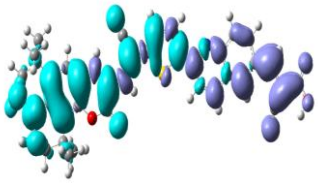	*L*=12.510 Ang Δ*e*=1.174 Ω= 0.120 *f*=1.695	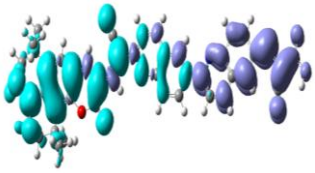	*L*=15.691 Ang Δ*e*=1.304 Ω= 0.040 *f*=1.430
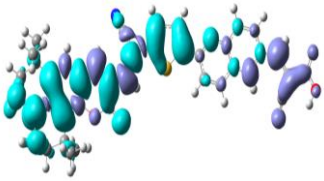	*L*=6.808 Ang Δ*e*=0.926 Ω= 0.682 *f*=0.577	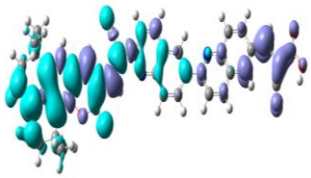	*L*=8.696 Ang Δ*e*=1.034 Ω= 0.510 *f*=0.668
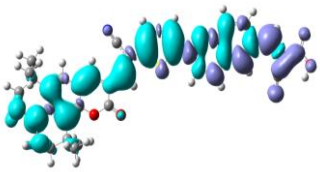	*L*=9.778 Ang Δ*e*=0.947 Ω= 0.348 *f*=0.293	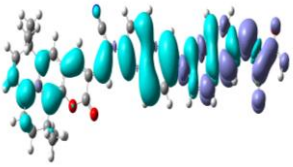	*L*=9.518 Ang Δ*e*=0.934 Ω= 0.352 *f*=0.541
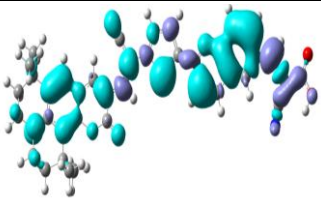	*L*=4.843 Ang Δ*e*= 0.689 Ω= 0.818 *f*=0.173	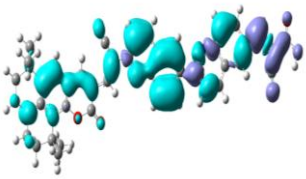	*L*=9.632 Ang Δ*e*=0.747 Ω= 0.364 *f*=0.145
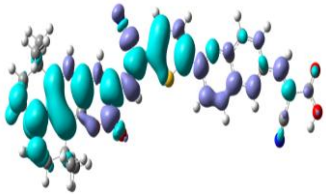	*L*=5.911 Ang Δ*e*=0.768 Ω= 0.721 *f*=0.156	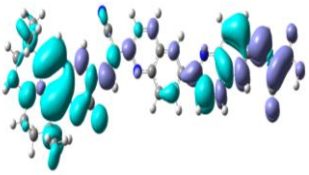	*L*=12.202 Ang Δ*e*=0.902 Ω= 0.388 *f*=0.128
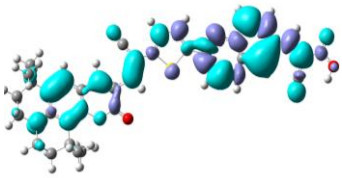	*L*=2.168 Ang Δ*e*=0.749 Ω= 0.856 *f*=0.309	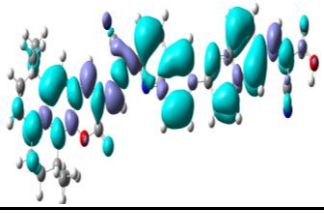	*L*=1.755 Ang Δ*e*=0.713 Ω= 0.951 *f*=0.137
		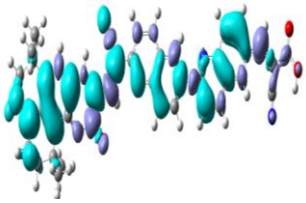	*L*=5.831Ang Δ*e*= 0.723 Ω= 0.823 *f*=0.103

	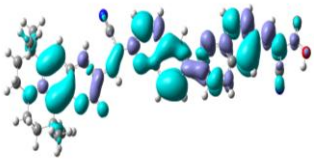	*L*=4.656 Ang Δ*e*=0.6509 *Ω*= 0.828 *f*=0.273

Table 15S Calculated HOMO, LUMO energy levels (eV) of all sensitizers and the HOMO, LUMO energy levels (eV) of the donor (coumarin343) and the acceptor (conjugated π-spacer and anchoring group) fragments of all sensitizer obtained by B3LYP functional

molecule	ε_{LUMO}	$\Delta\varepsilon_{HOMO-LUOMO}$	ε_{HOMO}
Coumarin343	-1.626		-5.267
frag-2311	-2.752		-7.256
frag-2677	-2.890		-5.967
frag-2677-P1	-3.054		-6.546
frag-2677-P2	-3.184		-6.586
frag-2700	-2.904		-5.660
frag-2700-P1	-3.081		-6.083
frag-2700-P2	-3.172		-6.569
frag-2883	-3.066		-5.979
frag-2883-P1	-3.207		-6.460
frag-2883-P2	-3.290		-7.084
frag-2883-Q1	-3.065		-6.193
frag-2883-Q2	-3.011		-6.297
NKX-2311	-2.693	2.614	-5.307
NKX-2677	-2.878	2.177	-5.055
NKX-2677-P1	-2.963	2.182	-5.145
NKX-2677-P2	-3.099	2.192	-5.291
NKX-2700	-2.896	2.071	-4.967
NKX-2700-P1	-3.049	2.010	-5.059
NKX-2700-P2	-3.110	2.143	-5.253
NKX-2883	-3.011	2.150	-5.161
NKX-2883-P1	-3.125	2.113	-5.238
NKX-2883- P2	-3.182	2.200	-5.382
NKX-2883-Q1	-3.017	2.164	-5.180
NKX-2883- Q2	-2.975	2.305	-5.280

Table 16S Calculated HOMO, LUMO energy levels (eV) of all sensitizers and the HOMO, LUMO energy levels (eV) of the donor (coumarin343) and the acceptor (conjugated π-spacer and anchoring group) fragments of all sensitizer obtained by M062X functional

molecule	ε_{LUMO}	$\Delta\varepsilon_{HOMO-LUOMO}$	ε_{HOMO}
Coumarin343	-0.758		-6.571
frag-2311	-1.749		-8.777
frag-2677	-2.051		-7.221
frag-2677-P1	-2.202		-7.870
frag-2677-P2	-2.302		-8.207
frag-2700	-2.246		-6.802
frag-2700-P1	-2.251		-7.37
frag-2700-P2	-2.311		-7.945
frag-2883	-2.219		-7.186
frag-2883-P1	-2.360		-7.727
frag-2883-P2	-2.423		-8.393
frag-2883-Q1	-2.245		-7.441
frag-2883-Q2	-2.201		-7.555
NKX-2311	-1.941	4.503	-6.444
NKX-2677	-2.132	4.062	-6.194
NKX-2677-P1	-2.144	4.100	-6.244
NKX-2677-P2	-2.384	4.001	-6.385
NKX-2700	-2.203	3.889	-6.091
NKX-2700-P1	-2.309	3.854	-6.164
NKX-2700-P2	-2.398	3.960	-6.358
NKX-2883	-2.337	3.963	-6.2996
NKX-2883-P1	-2.393	3.924	-6.3162
NKX-2883-P2	-2.492	3.954	-6.4460
NKX-2883-Q1	-2.356	3.972	-6.3282
NKX-2883-Q2	-2.301	2.600	-6.3962

Table 17S Molecular orbital composition (in %) of the highest occupied and two lowest unoccupied molecular orbital of the twelve coumarin sensitizers performed in ethanol solvent using B3LYP functional and the 6-31G(d,p) basis set.

system	orbital	Anchoring ligand	π-linker	C343
NKX-2311	HOMO	17	13	70
	LUMO	34	18	47
	LUMO+1	27	10	63
NKX-2677	HOMO	7	37	56
	LUMO	36	49	15
	LUMO+1	16	24	61
NKX-2677-P1	HOMO	4	32	64
	LUMO	42	45	13
	LUMO+1	16	19	66
NKX-2677-P2	HOMO	1	11	88
	LUMO	49	45	6
	LUMO+1	13	30	57
NKX-2700	HOMO	7	46	47
	LUMO	31	57	12
	LUMO+1	17	29	54
NKX-2700-P1	HOMO	5	36	59
	LUMO	41	50	10
	LUMO+1	19	28	53
NKX-2700-P2	HOMO	1	14	85
	LUMO	42	53	5
	LUMO+1	18	38	44
NKX-2883	HOMO	6	46	48
	LUMO	24	55	21
	LUMO+1	24	41	36
NKX-2883-P1	HOMO	2	38	60
	LUMO	33	52	15
	LUMO+1	22	37	41
NKX-2883-P2	HOMO	1	25	74
	LUMO	43	49	8
	LUMO+1	14	38	48
NKX-2883-Q1	HOMO	2	42	57
	LUMO	34	54	12
	LUMO+1	18	41	41
NKX-2883-Q2	HOMO	0	30	69
	LUMO	45	51	4
	LUMO+1	8	46	46

Table 18S Molecular orbital composition (in %) of the highest occupied and two lowest unoccupied molecular orbital of the twelve coumarin sensitizers performed in ethanol solvent using PBE0 functional and the 6-31G(d,p) basis set.

system	orbital	Anchoring ligand	π-linker	C343
NKX-2311	HOMO	16	13	70
	LUMO	34	19	47
	LUMO+1	27	10	63
NKX-2677	HOMO	6	36	58
	LUMO	36	49	14
	LUMO+1	16	24	60
NKX-2677-P1	HOMO	3	31	66
	LUMO	42	45	13
	LUMO+1	16	19	66
NKX-2677-P2	HOMO	1	10	89
	LUMO	49	46	6
	LUMO+1	14	30	56
NKX-2700	HOMO	6	45	49
	LUMO	32	57	11
	LUMO+1	17	29	53
NKX-2700-P1	HOMO	5	35	60
	LUMO	41	50	9
	LUMO+1	19	28	53
NKX-2700-P2	HOMO	1	14	86
	LUMO	41	54	5
	LUMO+1	18	38	43
NKX-2883	HOMO	5	45	50
	LUMO	24	55	21
	LUMO+1	25	40	35
NKX-2883-P1	HOMO	2	37	61
	LUMO	33	53	15
	LUMO+1	22	37	41
NKX-2883-P2	HOMO	1	24	75
	LUMO	43	50	8
	LUMO+1	14	38	47
NKX-2883-Q1	HOMO	1	40	58
	LUMO	34	55	11
	LUMO+1	18	41	41
NKX-2883-Q2	HOMO	0	30	70
	LUMO	44	52	4
	LUMO+1	8	47	45

Table 19S Calculated energy (a.u) of the oxidized coumarin dyes in ethanol solvent using PBE0 functional and the 6-31G(d,p) basis set

scheme	Dye^{+}	Dye^{+2}	ΔG(aq)
NKX-2311	-1376.9660	-1376.5874	10.3021
NKX-2677	-2402.6491	-2402.3104	9.2164
NKX-2677-P1	-2113.9945	-2113.6450	9.5102
NKX-2677-P2	-1825.3309	-1824.9602	10.0871
NKX-2700	-2479.9639	-2479.6372	8.8898
NKX-2700-P1	-2191.3100	-2190.9704	9.2409
NKX-2700-P2	-1902.6453	-1902.2898	9.6735
NKX-2883	-2572.0934	-2571.7594	9.0885
NKX-2883-P1	-2283.4424	-2283.0977	9.3796
NKX-2883-P2	-1994.7868	-1994.4233	9.8912
NKX-2883-Q1	-2420.8846	-2420.5487	9.1402
NKX-2883-Q2	-2269.6788	-2269.3410	9.1919

Table 20S Calculated energy (a.u) of the oxidized coumarin dyes in ethanol solvent using B3LYP functional and the 6-31G(d,p) basis set

scheme	Dye^{+}	Dye^{+2}	$\Delta G_{(aq)}$
NKX-2311	-1378.6084	-1378.3760	6.3235
NKX-2677	-2404.8416	-2404.6343	5.6453
NKX-2677-P1	-2116.1605	-2115.9437	5.9001
NKX-2677-P2	-1827.4690	-1827.2324	6.4385
NKX-2700	-2482.2532	-2482.0529	5.4527
NKX-2700-P1	-2193.5692	-2193.3594	5.7076
NKX-2700-P2	-1904.8791	-1904.6492	6.2550
NKX-2883	-2574.4878	-2574.2795	5.6675
NKX-2883-P1	-2285.8064	-2285.5885	5.9299
NKX-2883-P2	-1997.1241	-1996.8894	6.3867
NKX-2883-Q1	-2423.4130	-2423.2006	5.7796
NKX-2883-Q2	-2272.3441	-2272.1212	6.0667

Table 21S Calculated energy (a.u) of the oxidized coumarin dyes in ethanol solvent using M062X functional and the 6-31G(d,p) basis set

scheme	Dye^{+}	Dye^{+2}	$\Delta G(aq)$
NKX-2311	-1377.9520	-1377.5661	10.5007
NKX-2677	-2404.0415	-2403.6960	9.4014
NKX-2677-P1	-2115.3524	-2114.9952	9.7198
NKX-2677-P2	-1826.6550	-1826.2703	10.4681
NKX-2700	-2481.4114	-2481.0778	9.0776
NKX-2700-P1	-2192.7240	-2192.3762	9.4640
NKX-2700-P2	-1904.0244	-1903.6535	10.0926
NKX-2883	-2573.6186	-2573.2781	9.2653
NKX-2883-P1	-2284.9330	-2284.5806	9.5892
NKX-2883-P2	-1996.2431	-1995.8658	10.2667
NKX-2883-Q1	-2422.4781	-2422.1332	9.3851
NKX-2883-Q2	-2271.3406	-2270.9868	9.6273